Chapter 7
Groundwater Contamination and Induced Risk and Hazard in a Karst Aquifer

Studying and rehabilitating groundwater in hydrogeologic settings such as karst, fractured rock, and deep alluvial aquifer systems presents significant challenges. The process of restoring aquifers and developing accurate conceptual site models becomes even more complex due to various factors associated with contaminants. The coexistence of light non-aqueous phase liquids (LNAPLs) and dense non-aqueous phase liquids (DNAPLs) further complicates the selection of appropriate remedial response strategies. In order to assess the feasibility of restoration efforts, the National Research Council (NRC 1994) has categorized sites into different classes, as illustrated in Table 7.1.

The intricate nature of hydrogeologic conditions in karst terranes poses challenges for aquifer restoration efforts. The variations in porosity and hydraulic conductivity within these terranes make it difficult to predict changes in hydraulic head, groundwater flow, and contaminant transport. Typically, a small percentage of the aquifer volume accounts for the majority of water flow and contaminant migration. Therefore, targeting remedial actions towards these permeable pathways may enhance restoration effectiveness. However, identifying these significant transport zones in karst hydrogeologic settings can be challenging. Furthermore, complexities arise from vertical hydraulic connections that exist within multiple water-bearing formations, as well as the influence of groundwater production wells on the movement and direction of groundwater and contaminants.

Characterizing the distribution of contaminants, groundwater flow paths, and potential receptors in karst environments with open conduit flow poses significant challenges. Contaminants exhibit distinct behavior in karst aquifers compared to granular or fractured rock aquifers. Within karst aquifers, contaminants can be stored in the vadose zone and the contact zone between bedrock and overburden, known as the epikarst zone. Periodic recharge events, such as seasonal or storm-related influxes, can flush a part of the contaminants into the bedrock aquifer. Groundwater flow within the bedrock converges towards conduits, such as subterranean caverns, resulting in rapid flow over long distances towards receptors. It is important

P. Li et al., *Hazard Hydrogeology*, Environmental Earth Sciences,
https://doi.org/10.1007/978-3-031-48427-8_7

Table 7.1 Feasibility and relative ease of contaminated groundwater investigation and remediation (NRC 1994)

Hydrogeological properties	Properties of contaminants					
	Mobile and dissolved	Mobile and dissolved	Strongly sorbed and dissolved	Strongly sorbed and dissolved	Separate phase of LNAPLs	Separate phase of DNAPLs
Homogeneous, and single layers	1	1-2	2	2-3	2-3	3
Homogeneous, and multiple layers	1	1-2	2	2-3	2-3	3
Heterogeneous, and single layers	2	2	3	3	3	4
Heterogeneous, and multiple layers	2	2	3	3	3	4
Fractured and Karst	3	3	3	3	4	4

1 and 1-2	Achieving a full cleanup of aquifers to meet health-based standards is considered feasible based on current knowledge.
2, 2-3, and 3	The feasibility of achieving a complete technical cleanup is likely to be uncertain.
4	Currently, there are no available technologies capable of fully cleaning up aquifers.

to acknowledge that conventional groundwater flow equations may not accurately capture the turbulent flow dynamics present in karst environments. The presence of DNAPLs further complicates aquifer restoration, as specialized techniques are required to assess associated risks and hazards. To address these intricate challenges, this chapter presents a compelling case study that showcases the implementation of specialized techniques and innovative approaches for the assessment and mitigation of contaminated groundwater.

7.1 Investigation Approaches

The geological characteristics of the study area, which included karst-type lithologies, presented significant challenges in gathering the necessary data for hydrogeological characterization. Compared to aquifers in other hydrogeologic settings, the investigation in karst areas required tailored approaches that were typically conducted in phases (Teutsch and Sauter 1991). Figure 7.1 illustrates the various techniques employed in the remedial investigation of the specific karst site. A three-phase approach was utilized to characterize the site, and this section provides detailed descriptions of several techniques that were unique to this site-specific investigation. The presence of karst is indicated by the formation of distinct physiographic features that develop due to the dissolution of soluble limestone or dolomite beneath the surface. These features may include sinkholes, sinking streams, caves, and springs. The hydrological characteristics associated with karst environments are also unique and typically involve the following: (1) Internal drainage of surface runoff through sinkholes. (2) Diversion or partial subsurface flow of surface streams, known as sinking streams or losing streams. (3) Vertical structure comprising three zones: overburden, epikarst, and bedrock. (4) Bedrock aquifer characterized by triple-porosity, including pores, fractures, and conduits. (5) Release of subsurface water from conduits through one or more large and continuous springs. Karst aquifers

exhibit heterogeneity and possess hydraulic properties that vary depending on the scale of observation and may also change over time.

In areas with karst features, it is crucial to acknowledge that conventional hydrogeologic techniques alone, such as potentiometric mapping, hydraulic testing of monitoring wells, or numerical modeling, may not fully characterize the flow system. Gathering the necessary data often requires a phased and multidisciplinary approach that integrates specialized investigation methods. Some of these methods include:

Water-tracing tests: These tests involve introducing a tracer substance into the groundwater system and monitoring its movement to understand the flow paths and connections between different parts of the aquifer. Tracers can be dyes, fluorescent substances, or isotopes that can be detected and traced back to their source.

Digital geophysical mapping: Geophysical methods, such as electrical resistivity tomography (ERT) or ground-penetrating radar (GPR), can be used to map subsurface features and identify potential conduits, fractures, or voids within the karst aquifer. These techniques provide valuable information about the subsurface structure and can aid in understanding groundwater flow patterns.

Packer testing: Packer tests involve isolating specific sections of a borehole using inflatable packers and conducting aquifer tests to evaluate the hydraulic properties of the surrounding rock or aquifer. This method helps in characterizing the permeability and flow characteristics of different zones within the karst aquifer.

Multi-level groundwater monitoring: Installing multiple monitoring wells at different depths within the karst aquifer allows for the collection of data on water levels, water quality parameters, and flow velocities at various locations. This approach provides insights into the vertical and horizontal variations in groundwater flow and helps in understanding the complex hydrogeologic behavior of the karst system.

By incorporating these specialized investigation methods into the phased approach, a more comprehensive understanding of the karst aquifer can be achieved, enabling better characterization of the flow system and more effective management of groundwater resources in karst environments.

7.1.1 On-Site Mobile Laboratory Application to Investigating Contamination Distributions

Seventeen soil borings were advanced using direct-push technology (DPT). These borings were placed in the presumed hydrogeologically downgradient direction from the suspected contamination source. The objective of the soil boring activities was to obtain screening-level field groundwater data from an on-site mobile laboratory for preliminary assessment of the contamination plume and to determine locations for additional monitoring wells. A track mounted geoprobe rig was utilized to advance

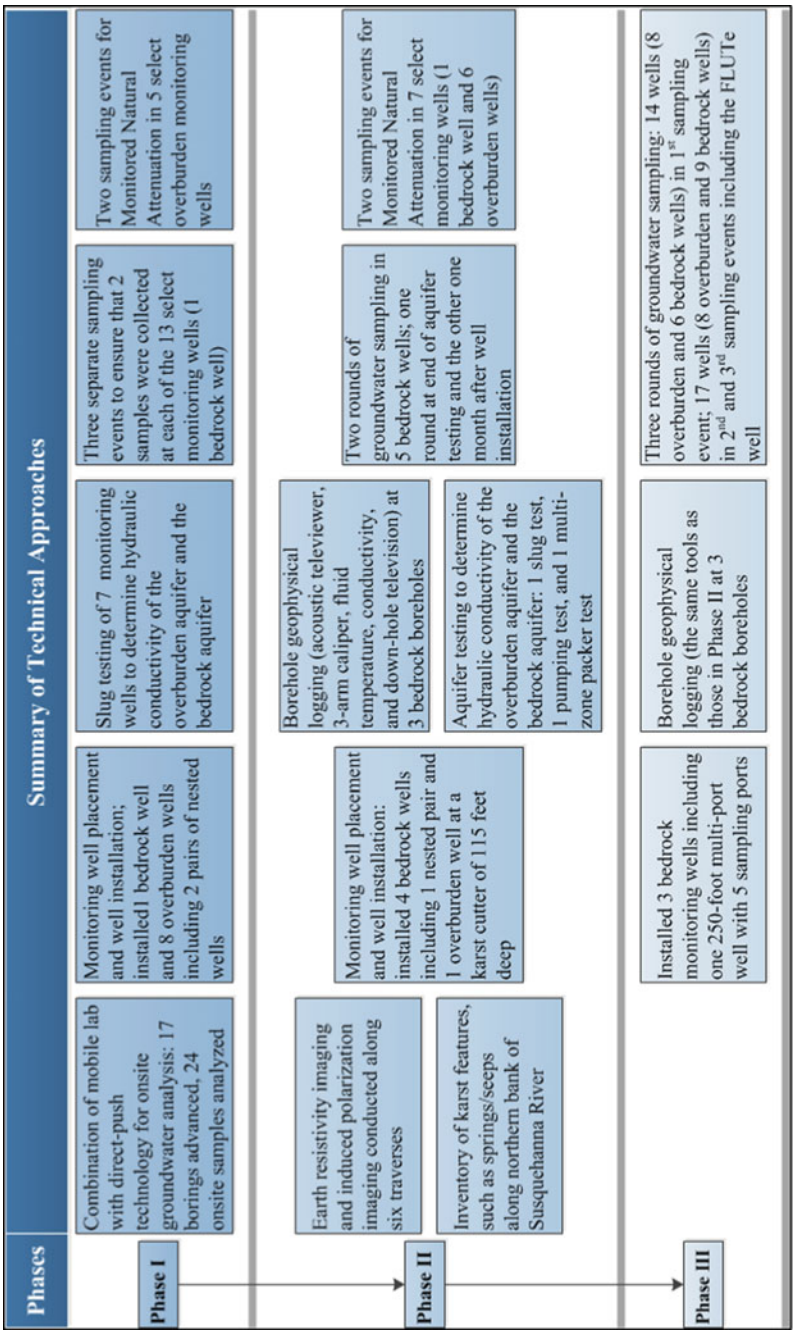

Fig. 7.1 Phased approach used in groundwater contamination investigation

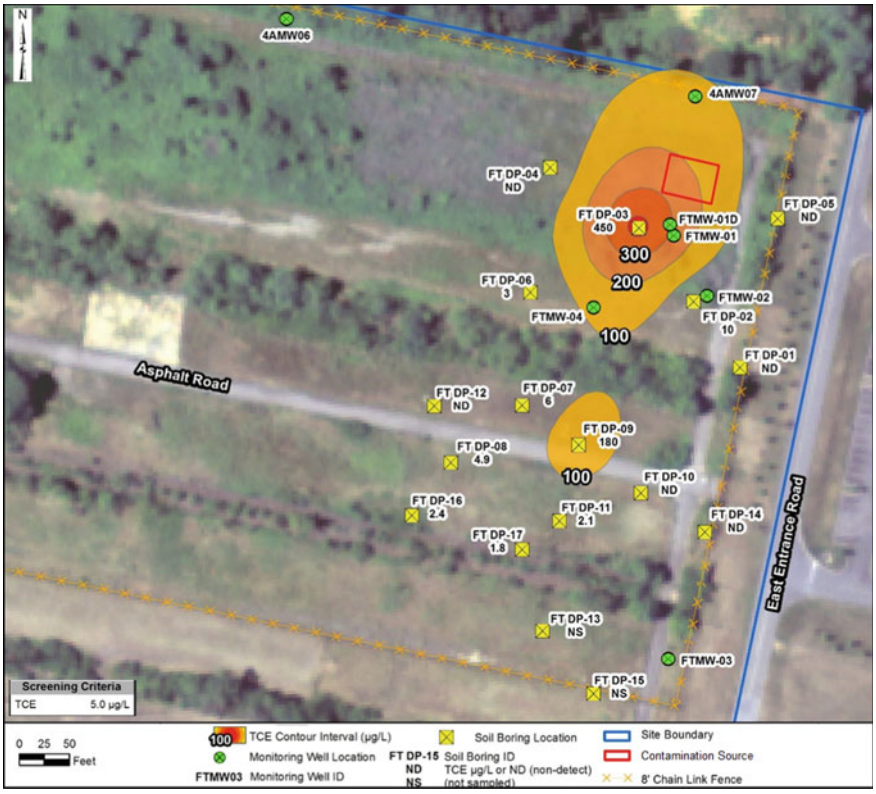

Fig. 7.2 TCE concentration distribution from on-site mobile laboratory analysis

each boring to refusal. Figure 7.2 shows the soil borings and the contours of the depth to refusal. The depth to refusal varied from 11 to 31 feet.

Groundwater was encountered above the refusal level at each boring. Upon advancement to refusal, the DPT tooling was extracted from the boring and offset to the side of the completed boring. The DPT macrocore sampler was exchanged for a discrete-depth groundwater sampler, and this was advanced next to the boring to just below the encountered groundwater. When this depth was reached, the discrete-depth groundwater sampler was partially retracted exposing the screened section. Single-use high density polyethylene tubing was inserted into the center of the Geoprobe rods and groundwater samples were collected by a peristaltic pump. The sample stream was collected in a laboratory-provided clean 20-milliliter (mL) volatile organic analysis vial. The sample was then transferred to the on-site mobile laboratory technician for analysis.

A mobile laboratory was set up for on-site screening level analysis of groundwater samples. Analysis was performed by direct injection gas chromatography analyses of the heated headspace of groundwater samples and target compounds were identified with the gas chromatograph's photoionization detector (PID) and

electron capture detectors. Tetrachloroethylene (PCE) and its degradation products including trichloroethylene (TCE) and cis-1,2-dichloroethene (cis-DCE) were targeted for detection. Table 7.2 presents the results from mobile laboratory analysis at geoprobe locations. Figure 7.2 also shows the TCE concentration distributions based on the on-site analysis data.

Table 7.3 compares the on-site analysis results with those by an in-house laboratory for two groundwater samples for quality assurance. Data in this table indicate that the TCE or cis-DCE results analyzed from the mobile laboratory may have underestimated the contamination concentrations. The on-site analysis results provide essential information on placing additional monitoring wells.

Table 7.2 Results of mobile laboratory analysis at geoprobe locations

Soil boring	Depth to refusal (feet below ground surface [bgs])	Results of mobile laboratory (μg/L)		
		TCE	cis-DCE	PCE
FTDP1	15.3	Non-detect (ND)	ND	0.1
FTDP2	31.0	10	67	0.087
FTDP3	17.0	450	450	0.46
FTDP4	16.5	ND	ND	0.13
FTDP5	15.0	ND	ND	0.075
FTDP6	20.0	3	0	0.075
FTDP7	30.0	6	2.9	0.093
FTDP8	23.0	4.9	3	0.1
FTDP9	27.3	180	620	0.49
FTDP10	34.8	ND	5.6	0.12
FTDP11	15.0	2.1	38	ND
FTDP12	20.0	ND	ND	ND
FTDP13	11.0	ND	ND	ND
FTDP14	18.5	ND	ND	0.15
FTDP15	11.8	ND	ND	ND
FTDP16	20.0	2.4	ND	ND
FTDP17	13.0	1.8	18	ND

Table 7.3 Quality assurance of on-site analysis

Analyte	FTMW-01		FTMW-04	
	On-site mobile laboratory (μg/L)	In-house laboratory (μg/L)	On-site mobile laboratory (μg/L)	In-house laboratory (μg/L)
TCE	150	850	65	120
cis-DCE	250	1700	53	120

7.1.2 *Earth Resistivity Imaging and Induced Polarization Imaging*

ERI (Earth resistivity imaging) and induced IP (polarization imaging) were conducted along six traverses. The objective of this geophysical survey was to investigate any subsurface fracturing and preferential groundwater flow pathways in the underlying dolomite to facilitate location of four new monitoring wells in bedrock. Figure 7.3 presents the location of the six ERI/IP traverses. The dipole–dipole array was used for the apparent resistivity and apparent IP data collection. The unit electrode spacing was 10 feet for all traverses. Fifty-six electrodes were used in all traverses, so the total length of each traverse was 550 feet.

Resistivity is a material property, and different materials, geological or otherwise, have different resistivity. The fundamental science behind application of ERI is the empirical Archie's law, which is often expressed by Eq. 7.1:

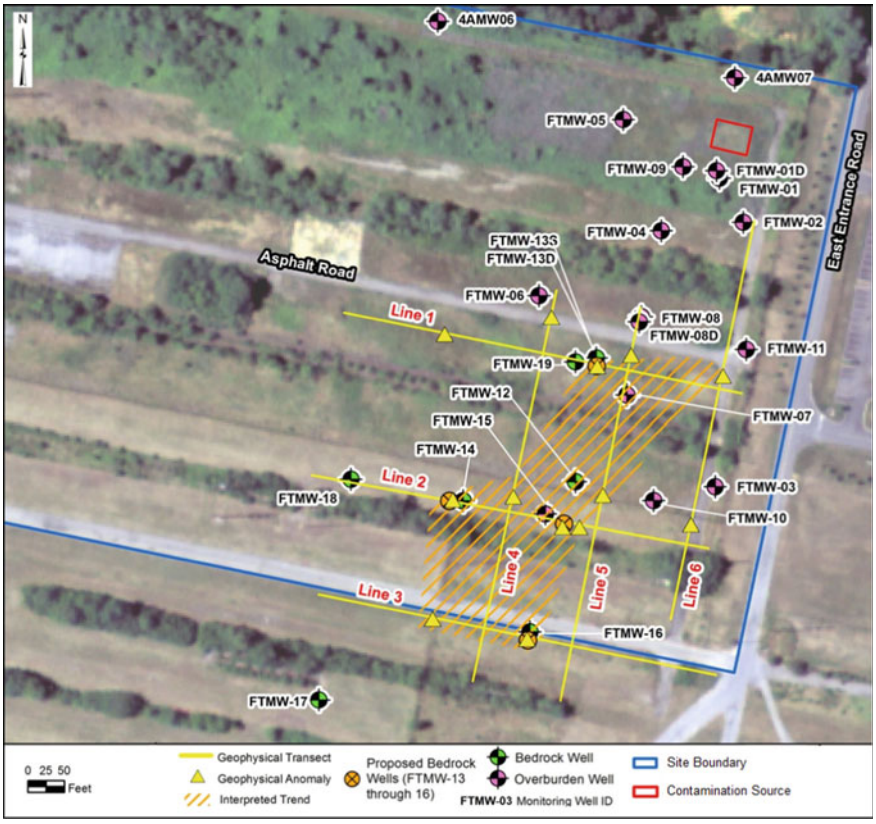

Fig. 7.3 Geophysical transects, interpretations, and proposed bedrock monitoring wells

$$\rho_0 = a\rho_w \phi^{-m} \tag{7.1}$$

where ρ_0 is the bulk resistivity for the soil/rock; ρ_w is the water resistivity; a is an empirical constant ($0.6 < a < 1$); m is the cementation factor ($m = 1.3$ for unconsolidated and $m = 2.2$ for cemented or crystalline), and ϕ is the fractional porosity, a ratio between water volume and soil/rock volume.

Both electrical resistivity and fractional volume of water in the earth materials are the main factors affecting the bulk resistivity. Large fractional volumes of water with low resistivity tend to correspond to overall resistivity lows, whereas dried materials tend to correspond to resistivity highs. Although bedrock such as limestone or dolomite may have high resistivity value, the bulk resistivity can be significantly decreased if the bedrock consists of large fractional volume of water. The resistivity of natural groundwater is typically low, and even lower if contaminated. Therefore, clay or water-filled fractures or conduits tend to have much lower resistivity values, while air-filled fractures or competent rock tend to have higher resistivity values. Table 7.4 lists possible resistivity values for materials encountered at the site.

The IP data were collected in conjunction with the ERI data. IP surveys involve measuring the polarization voltage magnitude that arises from injecting pulsed current into the ground, using the same instrument as electrical resistivity imaging (ERI). The integration of IP data aims to enhance the resolution and analysis of resistivity data in the following manners:

- Resolving thin stratigraphic layers can be improved by analyzing IP data, reducing some of the uncertainties encountered during electrical resistivity data modeling.
- IP data can aid in distinguishing geologic layers that may exhibit poor response in an electrical resistivity survey. The measurement of electrical chargeability, which is another physical property, can be utilized to augment hydrogeologic interpretations in various ways, such as distinguishing between equally electrically conductive targets like saline, hydrocarbon, or metallic-ion contaminant

Table 7.4 Possible interpretation of measured resistivity values

Value (ohm meter)	Interpretation
< 5	Possible interference from man-made objects (utilities) or artifacts from too many iterations in data processing
5–50	Clay dominated materials with high water content, saturated clay, clay-filled, or water-filled fractures or conduits
50–200	Moist silt, fine sand, weathered bedrock (dolomite) below water table
200–1000	Competent bedrock (dolomite), dry silty materials, possible small air-filled voids above water table
> 1000	Very competent rock (dolomite), dry sandy materials, possible large air-filled void above water table or artifacts from too many iterations in data processing

plumes and clay layers. This additional information can enhance the accuracy and effectiveness of the hydrogeologic interpretation.

There are two primary mechanisms attributed to the electrical chargeability or IP effect, although the exact causes are not yet fully understood. The first mechanism, known as electrode polarization or overvoltage effect, is predominant in rocks that contain metallic minerals. It occurs when conductive grains within the rock matrix hinder the flow of current, leading to the accumulation of charge on either side of these grains. When the current is removed, the ions responsible for the charge gradually diffuse back into the electrolyte (groundwater), causing the potential difference across each grain to decay slowly until it reaches zero. The second mechanism, known as membrane polarization, arises from the restriction of ion flow through narrow pore channels. It can also occur due to an excessive buildup of positive ions around clay particles. Exactly, the presence of a cloud of positive ions obstructs the movement of negative ions through the pores in the rock. When the applied voltage is removed, the concentration of ions gradually returns to its original state, resulting in the observed IP response. This phenomenon contributes to the electrical chargeability and is a key factor in understanding the IP effect.

During an IP survey, a square waveform is used to apply the current, and the polarization voltage is measured at short time intervals after each current cut-off. There is typically a brief delay of approximately 0.5 s before taking these measurements. These voltage readings are integrated to determine the area under the decay curve, which is used to define the voltage. To calculate the apparent chargeability, the integrated voltage is divided by the observed steady voltage. The observed steady voltage encompasses both the voltage resulting from the applied current and the polarization voltage. The apparent chargeability is expressed in milliseconds. By analyzing the measured apparent chargeability for a given charging period and integration time, qualitative information about the subsurface geology can be obtained.

Different minerals are distinguished by characteristic chargeabilities. However, it is challenging to use laboratory measurements to directly characterize the response of materials in the field because the IP response come from the processes of membrane polarizations caused by earth materials consisting of many minerals, and from electrode polarization caused by the presence of metallic grains. Both effects tend to be non-linear and depend on the surface area between the grains and fluids in the rock. Because minerals in groundwater can affect this interface, which may result in detectable changes in chargeability, the IP measurements can be applied to groundwater investigations. Table 7.5 lists typical chargeability of various earth materials.

Figure 7.4 shows the processed profiles on one of the geophysical lines (Line 2). Three graphs are presented. The top graph shows the modeled resistivity profile of the ERI; the middle graph shows the chargeability profile, and the bottom graph shows the normalized chargeability, which was obtained by dividing the chargeability by the resistivity. Fractures with groundwater flow and/or groundwater contamination typically have low resistivity and high chargeability. The interpreted anomalies

Table 7.5 Chargeability of various earth materials

Chargeability (milliseconds)	Materials
2000–3000	20% sulfides
1000–2000	8–20% sulfides
100–500	Sandstone, siltstone
50–100	Shale, clay
10–20	Limestone, dolomite
1–9	Sand, silt, gravel
0	Pure water
Variable, but can be in the thousands	Contaminated groundwater

are also plotted in Fig. 7.3. Based on the interpretation of resistivity and chargeability anomalies, the existing monitoring wells and the data gap in delineating the extent of bedrock contamination offsite, recommendations were made on additional monitoring wells.

The true resistivity/IP distributions along each traverse result from the measured apparent resistivity/IP data that are average values representing a volume of geologic material. The volume-averaged inherent in resistivity/IP methods tends to obscure small-scale irregularities in the geologic interfaces, except in very shallow subsurface. The data are more generalized at greater depths because of lower resolution due to averaging and/or smearing. Like other geophysical techniques, interpretation of resistivity/chargeability anomalies is not unique, especially in areas with complex geology such as the site. For example, isolated, near-surface areas of high resistivity may be caused by less moist silt, oxide nodules, or bedrock fragments. An apparent resistivity low may be caused by the presence of a clay- or water-filled fracture, cavity, or highly fractured but water-saturated rocks. A large void or multiple small voids may produce the same resistivity anomalies. Although the resistivity/IP imaging is two-dimensional, significant variations in subsurface resistivity in a direction perpendicular to the survey can cause distortions in the lower sections of the model (out-of-plane effects). This effect is most pronounced when the resistivity line is near a localized feature with different electrical properties than the material along the line (such as the railroad tracks at the site). Some of the resistivity/chargeability highs or lows shown on individual profiles may be caused by features that are actually laterally offset from the profile. As a result, when survey lines cross each other, the resistivity/chargeability profiles should be similar but may not be exactly the same at their intersections. The different results at the intersections may be indicative of the heterogeneous and anisotropic subsurface conditions.

When resistivity/IP data are interpreted, it is also important to understand how the image is created. The algorithm used in modeling is a “smoothing algorithm” meaning that a target is delineated by a number of equi-resistivity/chargeability lines. The lines describe the transition from one material to the other. However, if a target is too small, the equi-resistivity/chargeability lines will not reach the target values.

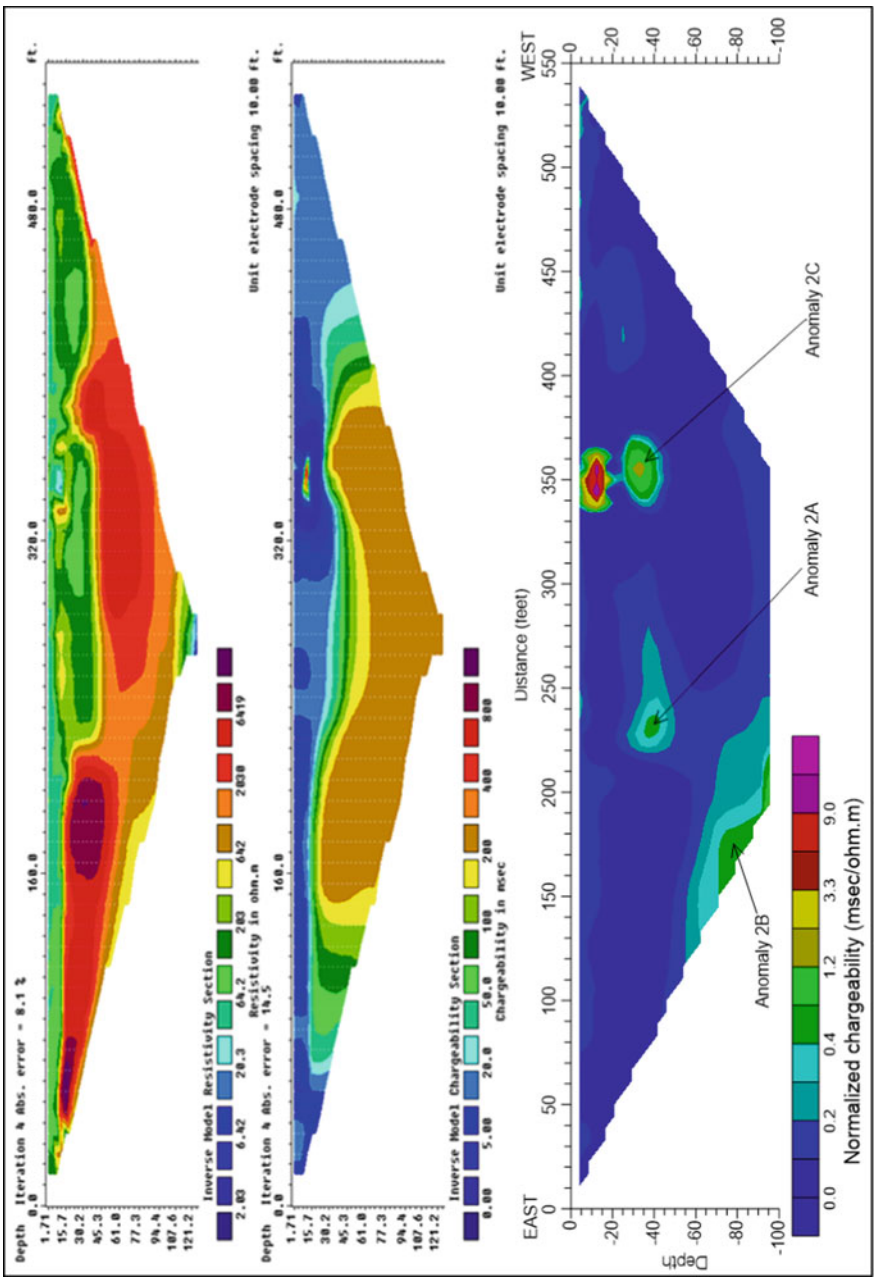

Fig. 7.4 Example image of normalized chargeability

Because the profiles are presented by resistivity/chargeability contours, the size of an anomaly over a geologic feature may be larger than the actual size of the feature.

7.1.3 Monitoring Well Installation and Aquifer Testing

Table 7.6 summarizes the monitoring wells installed during three phases and the associated investigation methods. Placement of these monitoring wells is based on location of suspected contamination area, on-site mobile laboratory analysis, and geophysical surveys. Monitoring well installation started with wells in the overburden and shifted to those in the bedrock. The boreholes were drilled using a combination of DPT, hollow stem auger (HSA) and air rotary drill. DPT or HSA was utilized to advance the boring through the alluvium overburden down to bedrock. The bedrock was then drilled using an air rotary drill rig. The formation characteristics were studied by the drilling logs, examining the cuttings, and a subsequent down-hole geophysical investigation in bedrock wells. The cuttings of each borehole were logged to the extent practicable to produce the drilling log. Visual observations such as depth of encountering water, voids, loss of circulation and changes in drill rig performance (i.e., rate of penetration) were recorded during the drilling process. The cuttings retrieved from the drilling were screened by a PID for volatile organic compounds (VOCs).

Aquifer characterization was conducted with slug test, pump test, and packer test. The slug used to perform the slug tests was made of polyvinyl chloride (PVC) cylinders and weighted internally with sand and concrete, with epoxy end caps and vinyl rope attached to each end. The slug has an outer diameter of 1.55 inches and 36 inches in length. The water level data were collected after lowering the slug into and pulling out of the water column. Prior to beginning the slug test, an initial water level measurement was collected. Initially, a pressure transducer was installed in the well to a depth below the target drawdown estimated for the test. Groundwater level data were collected for approximately 3 h prior to beginning the slug test. The transducer was set to collect data at one-minute intervals.

In packer testing, specific intervals within each borehole are isolated from the rest of the open bedrock borehole using straddle packer assemblies. These packers consist of external bladders coated with natural rubber, which are inflated with nitrogen to expand and create a seal against the borehole wall. By isolating these intervals, measurements of hydraulic head potential (water pressure) and yield (water flow) can be taken. The packer testing system typically includes a straddle packer assembly, a submersible pump, and a data collection system. Within each borehole, three pressure transducers calibrated to measure the depth to water are inserted as part of the straddle packer system. These transducers allow for continuous monitoring of water levels above, within, and below each isolated interval being tested. This comprehensive monitoring helps assess the hydraulic behavior and characteristics of the subsurface formations. The signals from the pressure transducers are transmitted through the top packer to a digital data logger. The data logger collects and records the measurements

Table 7.6 Summary of monitoring wells and associated investigations

Location ID	Screen interval (feet bgs)	Lithology	Total depth (feet)	Diameter (inches)	Aquifer testing	Borehole logging	Sampling and analysis	Groundwater level monitoring
4AM-07	5.9–24	Overburden	24	2			√	√
FTMW-01	5.9–20.9	Overburden	20.9	2	Slug test		√	√
FTMW-01D	79.6–99.6	Overburden	99.6	2			√	√
FTMW-02	5.8–20.8	Overburden	20.8	2			√	√
FTMW-03	7–22	Overburden	22	2			√	√
FTMW-04	4.6–19.6	Overburden	19.6	2			√	√
FTMW-05	11.5–16.5	Overburden	16.5	4			√	√
FTMW-06	15–25	Overburden	25	4	Slug test		√	√
FTMW-07	14–19	Overburden	19	4			√	√
FTMW-08	13–23	Overburden	23	4	Slug test		√	√
FTMW-08D	28–33	Overburden	33	4	Slug test		√	√
FTMW-09	15–25	Overburden	25	4	Slug test		√	√
FTMW-10	23.5–33.5	Overburden	33.5	4	Slug test		√	√

(continued)

Table 7.6 (continued)

Location ID	Screen interval (feet bgs)	Lithology	Total depth (feet)	Diameter (inches)	Aquifer testing	Borehole logging	Sampling and analysis	Groundwater level monitoring
FTMW-11	14–19	Overburden	19	4			√	√
FTMW-12	35–45	Bedrock	45	4	Slug test		√	√
FTMW-13S	19–34	Bedrock	34	2	Straddle packer test	ATV, 3-arm caliper, fluid temperature and conductivity, and down-hole television	√	√
FTMW-13D	55–70	Bedrock	70	2	Straddle packer test	ATV, 3-arm caliper, fluid temperature and conductivity, and down-hole television	√	√
FTMW-14	40–55	Bedrock	55	2	Pump test	ATV, 3-arm caliper, fluid temperature and conductivity, and down-hole television	√	√
FTMW-15	108–128	Overburden	128	2	Slug test		√	√
FTMW-16	16–40 open hole, 40–47 gravel pack	Bedrock	47	6	Straddle packer test	ATV, 3-arm caliper, fluid temperature and conductivity, and down-hole television	√	√
FTMW-17	38–68	Bedrock	68	6			√	√
FTMW-18	18–48	Bedrock	48	6			√	√

(continued)

Table 7.6 (continued)

Location ID	Screen interval (feet bgs)	Lithology	Total depth (feet)	Diameter (inches)	Aquifer testing	Borehole logging	Sampling and analysis	Groundwater level monitoring
FTMW-19 Zone 1	96.4–106.4	Bedrock	106.4	6		ATV, 3-arm caliper, fluid temperature and conductivity, and down-hole television	√	√
FTMW-19 Zone 2	124.9–130.9	Bedrock	130.9	6			√	√
FTMW-19 Zone 3	137.9–143.9	Bedrock	143.9	6			√	√
FTMW-19 Zone 4	188.9–193.9	Bedrock	193.9	6			√	√
FTMW-19 Zone 5	226.9–231.9	Bedrock	231.9	6			√	√

of water levels from the transducers. The output from the data logger is then directed to a field laptop computer, where the data can be analyzed and further processed. A pump test was conducted at FTMW-14 in which a highly permeable zone was encountered approximately 20 feet into the bedrock after auger refusal and drilling was difficult because of high water production in the formation. Monitoring well FTMW-14 was pumped at a constant rate of 11.5 gallons per minute (gpm) for approximately 2.6 h for the pump test. Prior to the pumping test, pressure transducers were installed in the pumped well and in three existing monitoring wells (FTMW-13, FTMW-15, and FTMW-16), which were used as observation wells during the pumping test.

Borehole geophysical logging, including acoustic televiewer (ATV), 3-arm caliper, fluid temperature and conductivity, and down-hole television, was performed at bedrock wells to identify relevant characteristics of the boreholes and determine fracture intervals and water production zones.

7.1.4 Borehole Logging and Design of Multi-port Monitoring Well

Borehole geophysical logging, including ATV, 3-arm caliper, fluid temperature and conductivity, and down-hole television, was performed at bedrock boreholes including the multi-port monitoring well FTMW-19. The purpose of this investigation was to identify relevant characteristics of the boreholes and determine the appropriate spread interval for the packer testing. The total depth of the well is approximately 260 feet below the top of the casing. The measurement from the top of the casing to the land surface is 1.10 feet. The well is constructed with a 5-inch diameter steel casing, which is set to a depth of approximately 91.5 feet below the top of the casing. This means that the open borehole interval, where the packer testing is conducted, spans from 91.5 feet below the ground surface (bgs) to approximately 260 feet bgs. At the time of the survey, the depth-to-water level in the well was approximately 18.3 feet below the top of the casing. Figure 7.5 displays a portion of the logging data obtained from the borehole at FTMW-19.

Caliper (3-arm): The caliper log is a tool used to measure and record the average diameter of a borehole. It provides information about changes in borehole diameter that are associated with well construction, such as the depth of the well casing or the location of a screened interval. Additionally, the caliper log is valuable in identifying potential fracture zones in open bedrock wells. The caliper log consists of three spring-loaded feeler arms that work together to determine the average diameter of the borehole. Before collecting the caliper logs, the tool is calibrated at the surface using measuring templates. It is then lowered into the borehole to the desired depth, and the feeler arms are remotely opened. The logging process involves moving the caliper tool in an upward direction within the borehole. Ten (10) inflections representing an increase in the average borehole diameter were identified. The top of the inflections

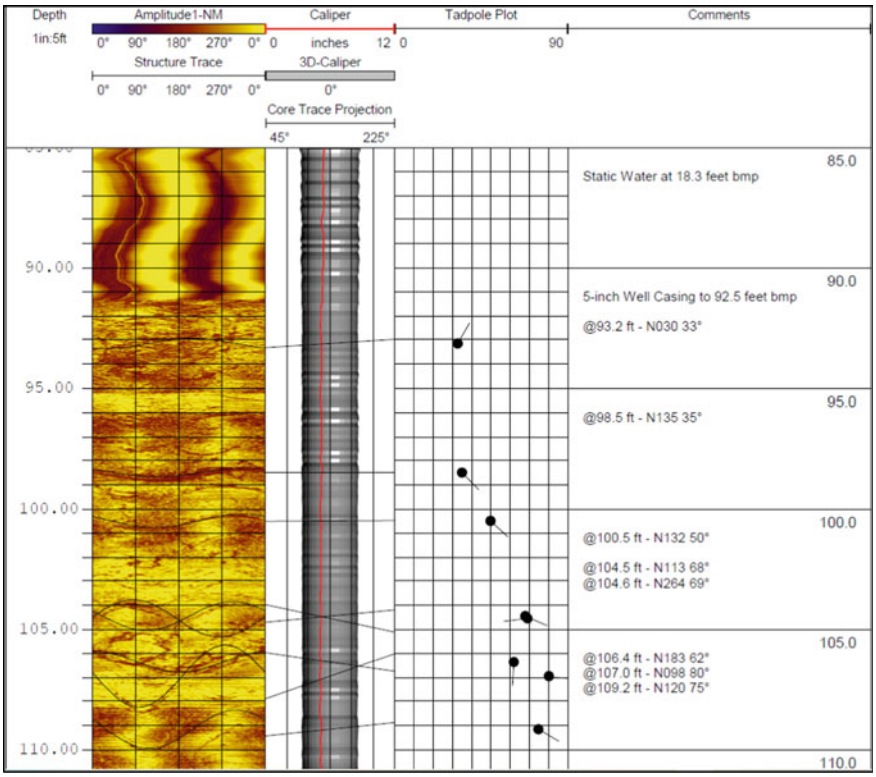

Fig. 7.5 Part of geophysical logs for FTMW-19

was found at 98, 109, 115, 126, 132, 145, 149, 178, 195, and 248 feet bgs. Based on the size of the inflections in the caliper log all these features represent minor increases in the average borehole diameter.

Acoustic televiewer: The acoustic televiewer (ATV) is a tool used for borehole imaging that functions similarly to a borehole television survey. It generates a 360° image of the borehole, but instead of relying on light, it uses a focused beam of ultrasound to produce the image. It is important to note that the ATV can only provide data in the fluid-filled portion of the borehole. It is unable to produce images in dry or partially filled sections of the borehole. The ATV records both the amplitude and the delay in transit of the reflected ultrasound signal, also known as travel time. These measurements provide valuable information about the borehole conditions, including the reflectivity of the surrounding rock and the size of the borehole.

The ATV printout contains information obtained from the survey of the borehole using the acoustic televiewer. It includes several graphics and a comments field that provide important details about the borehole features. The first graphic on the ATV printout is the borehole televiewer amplitude log, which is represented as an

"unwrapped core" displayed from North to North. The N45°-N225° graphic represents the apparent angle of the borehole through a "3-D" representation. The borehole image is viewed from a position that is rotated counter-clockwise by 45°. The arrow plot in the ATV printout displays the feature angle (ranging from 0 to 90°) and the direction of dip. It uses a "tadpole" symbol to indicate the features, with the angle of the feature represented by the position of the tadpole's head, and the tail pointing in the direction of dip. The comments field in the ATV printout lists additional information about the identified features. A diagonal pattern wrapping from the north side of the image appears on the ATV log starting at a depth of 119 feet bgs. Based on the down-hole television survey and the caliper log it appears that a slight change in the size and smoothness of the borehole also occurs at this depth. This change may be due to a possible drill bit change and/or the combination with a facies change in the characteristics of the bedrock below the depth of 119 feet bgs. The ATV log produced for the well was analyzed and twenty-one (21) features were identified based on correlation with inflections in the caliper log. Table 7.7 lists the characteristics for each feature identified in the ATV log.

Fluid temperature and conductivity/resistivity: The fluid temperature log is used to measure the temperature of the surrounding air, water, or formation within the borehole. Abrupt changes in the slope of the temperature log can indicate the presence of water with different temperatures and/or quality entering or exiting the borehole. The fluid conductivity log, on the other hand, measures the borehole fluid's electrolytic conductivity, typically reported in microSiemens per centimeter (μs/cm). In general, water with lower concentrations of TDS will result in lower fluid conductivity values, while water with higher amounts of total dissolved solids will exhibit higher conductivity values. Water quality can have an impact on fluid conductivity, and if sufficient details about specific contaminants in a well are available, the fluid conductivity log can provide valuable insights. By analyzing the fluid conductivity values alongside knowledge of certain contaminants, it becomes possible to draw conclusions about the composition of the borehole fluid. Changes observed in the fluid conductivity log can indicate variations in the borehole fluid when water-producing fractures or formations are transmitting fluid with different compositions into or out of the well. Fluid conductivity is the inverse of fluid resistivity. Typically, the fluid conductivity log is the initial parameter to be measured and is collected concurrently with the temperature log. Ten (10) inflections representing a change in temperature and/or resistivity were identified. The inflections are found at 98, 117, 128, 132, 157, 188, 200, 220, 240, and 248 feet bgs. The inflection depths correlate well with the caliper and ATV logs indicating possible zones of secondary porosity.

Down-hole television survey: During the down-hole television survey it was noted that the water clarity was fair (slightly cloudy) down to the bottom of the borehole at a depth of 260.5 feet. The open borehole consisted primarily of competent rock with calcite veins throughout. A fracture/weather zones that correlate well with the caliper, ATV, and fluid temperature/resistivity logs are visible at the depths of approximately 92–98 feet, 106–109 feet, 115–117 feet, 126 feet, 132 feet, 139 feet, 144 feet, 147 feet, 149.5 feet, 162 feet, and 178 feet.

Table 7.7 Acoustic televiewer features for well FTMW-19

Depth (feet bgs)	Feature		
	Strike azimuth (0–360°)	Feature dip azimuth (0–360°)	Dip angle (degree from horizontal)
93.2	300	30	33
98.5	45	135	35
100.5	42	132	50
104.5	23	113	68
104.6	174	264	69
106.4	93	183	62
107.0	8	98	80
109.2	30	120	75
115.9	68	158	62
126.5	53	143	68
128.9	51	141	59
131.8	52	142	66
139.0	54	144	70
144.0	41	131	76
149.3	177	267	59
153.4	192	282	47
161.8	54	144	77
177.8	86	176	65
191.0	56	146	65
194.8	33	123	71
230.5	141	231	59

FLUTe monitoring well design and installation: Unlike traditional groundwater monitoring wells, a FLUTe well uses flexible liner underground technologies to facilitate construction of multiple sampling ports in one well. A total of five sample ports were installed in the FLUTe monitoring well and were custom designed based upon field observations, and borehole logging, to align each port in fracture zones within the bedrock. The depths of the intervals for the five discrete sampling zones are:

- Zone 1 (FTMW-19-Z1), 96.4–106.419 feet
- Zone 2 (FTMW-19-Z2), 124.9–130.9 feet
- Zone 3 (FTMW-19-Z3), 137.9–143.9 feet
- Zone 4 (FTMW-19-Z4), 188.9–193.9 feet
- Zone 5 (FTMW-19-Z5), 226.9–231.9 feet

Upon determining the discrete sampling zones, a unique FLUTe sample liner was fabricated, to include the desired discrete sampling zones and a tubing bundle.

The installation of the FLUTe consisted of placing the unique form-fitting urethane coated nylon fabric liner within the borehole; the main component of the FLUTe monitoring well is the liner. The sample liner supports and seals the borehole. This method of installation allows for controlled installation whether horizontal, vertical, constricted, or curved. Typically, the sample liner descends by filling the inner portion of the liner with potable water provided by an off-site source, unrolling the sample liner from its shipped condition, and allowing the inherent water pressure securing the sample liner firmly into place against the borehole wall. A tether was attached to the sample liner to allow for controlled installation, but also for potential future removal of the sample liner. Figure 7.6 shows the installation and completion processes of the FLUTe well.

7.2 Hydrogeological Characterization

The formation of karst in carbonate rocks is predominantly linked to the dissolution of calcite in limestone and dolomite in dolostone. Various factors contribute to the karstification process, including the lithology of the bedrock, hydrogeology, bedrock structure, topography, climate, vegetation cover, time, and geological history. The initial step in the dissolution of carbonate rock involves the formation of carbonic acid, a mild acid formed when CO_2 dissolves in pore water. When rainfall descends and infiltrates the soil, it absorbs CO_2 from the atmosphere and the soil itself, which can contain elevated levels of CO_2 generated by the decomposition of organic matter. Consequently, the recharge water undergoes a transformation, becoming a diluted solution of carbonic acid. This acidified water permeates through the soil and eventually reaches the carbonate rocks. Guided by gravity, it continues its downward trajectory, traversing interconnected pores, fractures, or bedding planes within the rock. As the mild carbonic acid descends, it gradually dissolves and enlarges the preexisting pores or cracks, commonly known as "joints," through which it passes. Most near-surface rocks exhibit a dense network of joints, forming a complex pattern of intersecting cracks. While these joints can be widened through the process of dissolution, the majority of them do not extend to significant depths, typically only penetrating a few layers of rock or reaching depths of a few tens of feet. Once solution widening occurs, these joints have the ability to facilitate the movement of water. However, due to their limited vertical extent, the water cannot continue its downward flow. Solutionally widened fractures or joints are known as karren. These karren can vary in size, ranging from small seams to large, cavernous openings found at greater depths. On the irregular surfaces of the rock, undissolved rock formations, known as pinnacles, alternate with deep fractures that have been widened through solution. These widened fractures are often filled with clay, and they are commonly referred to as "cutters." Terzaghi and others (1996) state that, "the weathering products of limestone, dolomite and marble consist almost entirely of the insoluble portion of the parent rock. They usually form a nearly structureless residuum, generally clayey

Fig. 7.6 FLUTe well installation and completion

but sometimes sandy or pebbly, with no transition to the undissolved, unweathered rock. However, although sharp, the contact may be extremely irregular."

In contrast to the majority of joints, there are certain prominent cracks known as master joints that extend continuously through multiple layers of rock. These master joints play a crucial role in facilitating the downward movement of water to greater depths. When two master joints intersect vertically, they create a favorable pathway for water flow. This specific linear zone experiences faster dissolution compared to the surrounding areas due to the increased water volume it carries. As this zone enlarges, it becomes capable of transmitting larger quantities of water, diverting drainage from

the surrounding rock mass. This self-amplifying process leads to the formation of a few significantly enlarged tubes or pipes that penetrate through the carbonate rock, with minimal dissolution occurring between them, except in the upper portion of the carbonate rock.

The dissolution of carbonate rock is most rapid at the surface, where the water initially contacts the rock, as it is at its highest acidity during this stage. However, as the water infiltrates deeper into the bedrock, its acidity gradually diminishes, leading to a decrease in the dissolution rate. As a result, the upper portion of the carbonate rock undergoes extensive weathering and dissolution, particularly along joints and bedding planes (the horizontal surfaces between rock layers). This process gives rise to a complex network of interconnected planar features in three dimensions. This highly weathered and permeable zone, known as the epikarstic zone, is typically limited to the upper few tens of feet of the bedrock. Within the epikarst zone, water flow tends to converge towards drainage shafts, causing intensified dissolution and lowering of the rock in the vicinity of these shafts. This localized dissolution creates depressions in the carbonate rock, referred to as solution sinkholes. However, the visibility of these solution sinkholes depends on whether the bedrock is exposed at the ground surface, with minimal or no soil cover. Under certain circumstances, ongoing erosion of surface sediment can lead to the formation of a wide depression where the bedrock shaft becomes exposed at the base. This shaft can either be open, leading into a cave, or sealed with debris. In cases where the shaft is sealed, this condition is typically temporary and unstable. Eventually, the seal will be breached, and the erosion and subsidence process will resume. In some instances, sinkholes can be buried, meaning that solution or collapse sinkholes become filled with soil or sediment due to a change in the environmental conditions. As a result, there is no visible surface expression of these buried sinkholes.

The interplay between water circulation and rock dissolution in karst aquifers results in heterogeneity and anisotropy, where the extent of water circulation directly influences the degree of rock dissolution. As a consequence, the aquifers exhibit a combination of matrix voids, fractures, and caverns. Matrix voids refer to interconnected pores and vugs that store water and allow for laminar Darcian flow, where the viscosity and pressure of the fluid decrease as it moves through a porous medium over a given distance. Fractures in karst aquifers typically consist of joints, discontinuities, and bedding planes with a width of less than 1 cm. Water flow through these discrete fractures is often laminar, but it can transition to turbulent flow if there is a high hydraulic gradient, indicating a significant change in water pressure over a given distance. Caverns are formed through the dissolution of these fractures within the karst aquifer. They encompass enlarged fractures that exceed 1 cm in width, as well as conduits, caves, and underground rivers. The flow of water within these caverns resembles surface water flow and can become turbulent during recharge events when there is a substantial influx of water. It is important to recognize that groundwater flow within the karst aquifer can exhibit significant variability. While conduits and caves facilitate the movement of large volumes of water, there can also be areas of massive and impermeable rock with low hydraulic conductivity, impeding water transmission. These less permeable zones can be located in close proximity to areas

with high water storage capacity, resulting in a complex distribution of groundwater within the karst system.

7.2.1 Groundwater Flow

Figure 7.7 shows the layout of monitoring wells and general groundwater flow conditions. Based on the layout of monitoring wells and the observed groundwater flow conditions, it has been determined that the overburden formations have a hydraulic connection with the bedrock formations at the site. Both confined (where the aquifer is sandwiched between impermeable layers) and unconfined (where the aquifer is exposed to the surface) conditions exist in both the overburden and the bedrock aquifers. There was no hydrological barrier in the boreholes that would divide the groundwater flow in the overburden and the bedrock. The groundwater levels in the overburden and bedrock wells have a relatively uniform hydraulic gradient across the site. This uniform gradient suggests a good hydraulic connection between the overburden and the bedrock, allowing water to flow freely between the two. The average hydraulic gradient, measured at 0.015, indicates a southward flow towards the local river. This indicates that the groundwater is moving in a consistent direction, likely influenced by regional topography and hydraulic gradients. It is expected that the hydraulic connection can be enhanced a lot at the bedrock level due to the presence of a pinnacle-and-cutter bedrock surface. This type of bedrock surface typically exhibits irregularities and channels that can enhance the connectivity and flow of groundwater within the bedrock aquifer. These features promote the exchange of water between the overburden and the bedrock, further supporting the hydraulic connection observed at the site.

To determine the vertical gradients at the site, groundwater levels were measured in paired or clustered wells that are open to different depths. Several well pairs were utilized for this purpose, including FTMW-01 (shallow) and FTMW-01D (deep), FTMW-08 (shallow) and FTMW-08D (deep), and FTMW-13S (shallow) and FTMW-13D (deep). The measurements of hydraulic heads at FTMW-01 and FTMW-01D consistently showed higher groundwater elevations at FTMW-01. This indicates the presence of a vertical hydraulic gradient in this well pair, with groundwater flowing from the deep well (FTMW-01D) to the shallow well (FTMW-01). The consistent trend in hydraulic head measurements suggests a relatively stable flow pattern in this particular pair of wells. On the other hand, the measurements recorded at FTMW-08 and FTMW-08D, another pair of overburden monitoring wells, did not exhibit a similar consistency in hydraulic head measurements as observed in FTMW-01 and FTMW-01D. This suggests that the vertical hydraulic gradient in this well pair may be more variable or less pronounced compared to FTMW-01 and FTMW-01D. The hydraulic head measurements taken in October 2008 and December 2008 revealed that the groundwater table at FTMW-08 was lower than the groundwater table at FTMW-08D. This observation indicated an upward flow of groundwater in

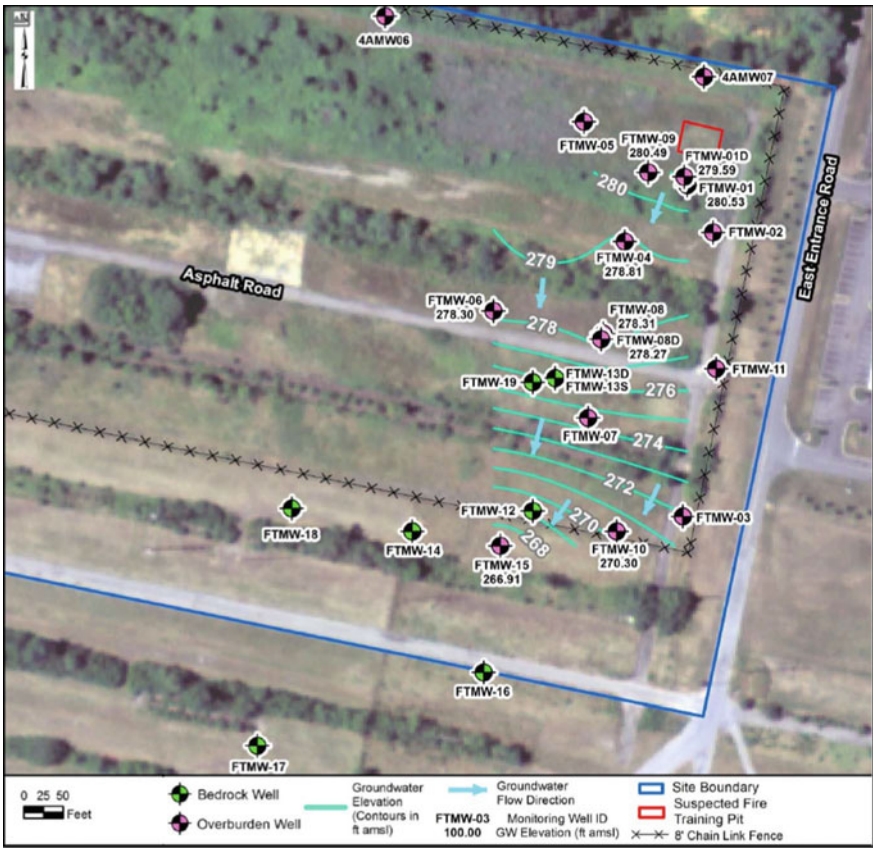

Fig. 7.7 Monitoring well layout and groundwater flow in overburden aquifer

this specific timeframe. However, subsequent measurements taken after 2008 indicated a different hydraulic head pattern. The measurements showed that the groundwater table at FTMW-08 was higher than the groundwater table at FTMW-08D. This change in hydraulic head suggested a downward flow of groundwater.

Alternatively, data collected from the nested bedrock wells FTMW-13S and FTMW-13D showed a different hydraulic head pattern. In 2012 and 2013, the measurements indicated that the groundwater table at FTMW-13S was lower than the groundwater table at FTMW-13D. This observation suggests an upward flow of groundwater in this specific area. The data further suggests that in the northern part of the site, a dominant downward flow pattern is present. This downward flow may have played a role in transporting the constituents of potential concerns (COPCs) to deeper portions of the overburden and potentially laterally into the bedrock formation. At the center of the site, the flow pattern can vary, with both downward and upward flow possibilities. This variable flow pattern may have implications for the movement and distribution of COPCs within the groundwater system.

The groundwater elevation levels measured at FTMW-19 showed a distinct pattern in five zones. Zone 1 had the highest groundwater table, while the levels gradually decreased as it moved towards zone 5, which had the lowest groundwater levels. This observation of decreasing hydraulic head from zone 1 to zone 5 is indicative of a downward flow of groundwater in this specific area.

As the groundwater flows towards a local river, there is a transition in flow patterns at the southern part of the site. In this area, the upward flow becomes dominant, indicating that groundwater is being discharged into the river. This change in vertical gradient suggests that the river serves as the point of discharge for groundwater at the site. However, it is worth noting that during field reconnaissance along the northern bank of the river, no springs or seeps were observed.

7.2.2 Irregular Bedrock Surface

Figure 7.8 depicts a hydrogeological cross-section from north to south, showing two layers: overburden materials and bedrock. The overburden materials are composed of silt and clay, with some likely formed from the weathering of residual material from carbonate bedrock. One notable observation is the significant variation in depth to bedrock over a short distance along the cross-section. The depth to bedrock ranges from 13 to 129 feet below ground surface (bgs), which corresponds to approximately 280–160 feet above mean sea level (amsl). FTMW-15 and FTMW-1D are located at bedrock cutters where the overburden thickness exceeds 100 feet. These features may represent buried sinkholes that were formed in the past and subsequently eroded into the surrounding bedrocks. Furthermore, the bedrock elevation at FTMW-12, which is approximately 60 feet north of FTMW-15, is 116 feet higher than that at FTMW-15, resulting in a steep slope of 2 to 1. The presence of bedrock lows creates direct lateral contacts between the bedrock and overburden. At FTMW-16, a cavity was encountered at a depth of 59 to 61.5 feet below ground surface (bgs), and the cavity was filled with mud and silt. During drilling, approximately five drums of mud were generated as a result of encountering this cavity. Above the cavity, competent rock was observed at a depth of 43 feet. However, within the 43 feet of competent rock, low water productivity was exhibited. At FTMW-10, a layer of sand and silt measuring 9 feet in thickness observed between 26 and 35 feet bgs was encountered between the bedrock. The presence of the sand and silt layer indicates dissolution or erosion of the bedrock in that area. Similarly, the 5-port well FTMW-19 encountered voids between 78 and 79 feet bgs. These voids were filled with clay and sand. Figure 7.9 shows the irregular bedrock surface elevation configuration.

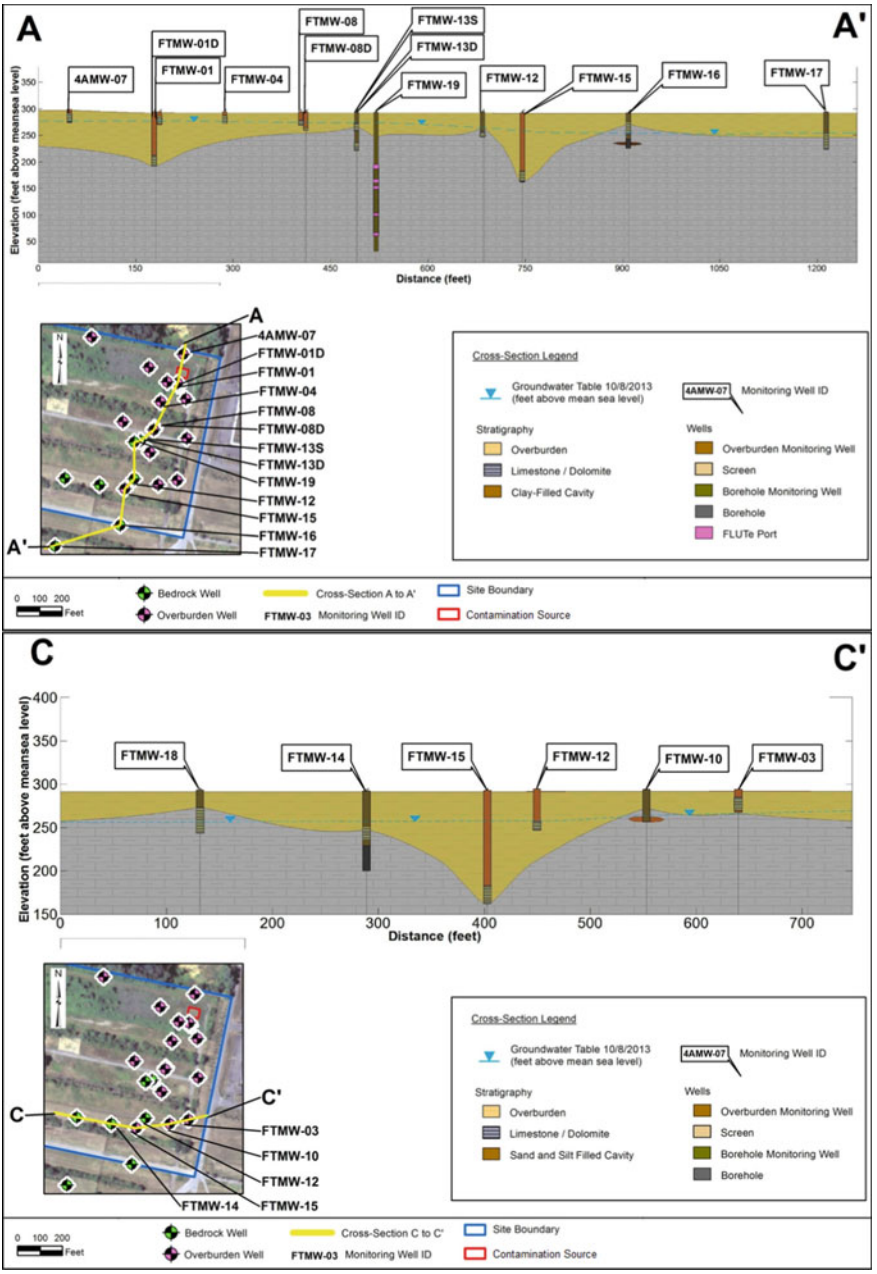

Fig. 7.8 Two-layer hydrogeological cross-sections (overburden and bedrock)

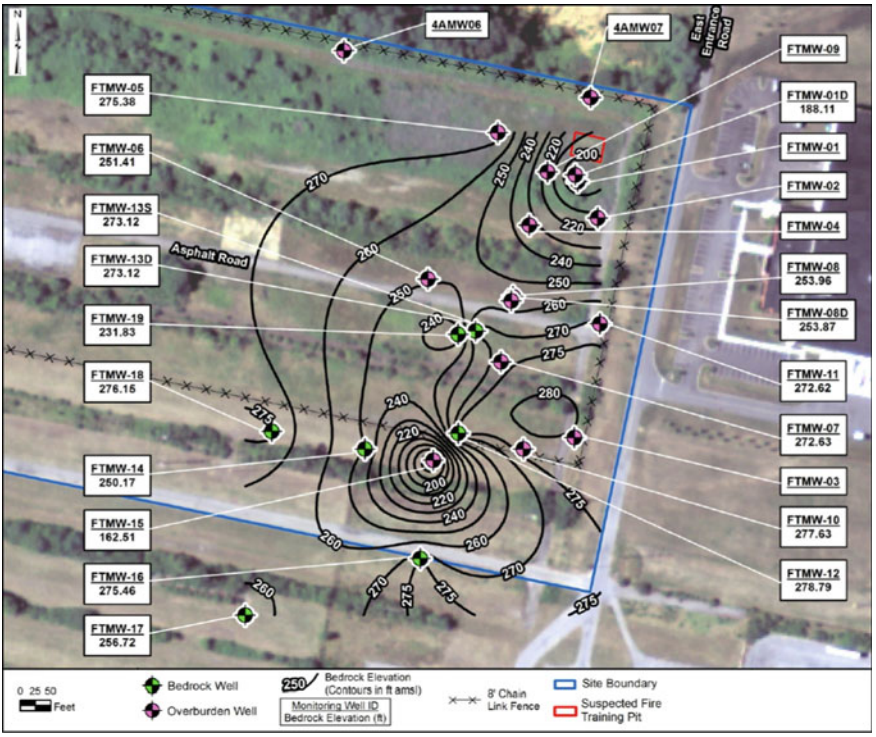

Fig. 7.9 Bedrock elevation contours

7.2.3 Unstable Boreholes

The encountered unstable boreholes and the presence of rounded gravel and cobbles at FTMW-14 indicate that this well is in a transmissive path for groundwater. The rounded nature of the quartz and dolomite cobbles indicates that they have been transported and shaped by water, further supporting the idea of a productive zone in this well. The unstable borehole at FTMW-19, where the casing was pushed in to prevent falling fragments of fractured dolomite, indicates the presence of fractured rock within the bedrock formation. At FTMW-13, discrete fracture zones were observed, indicating distinct areas of fractured rock within the bedrock. Borehole logging conducted at this well revealed jaggy borehole walls and the presence of water flow through three distinct fracture zones at different depths. These fracture zones were observed between 19 and 71 feet below ground surface (bgs). The packer tests showed that pumping at one zone produced simultaneous drawdowns at the other zones, indicating hydraulic interconnection between these fracture zones. Similarly, at FTMW-19, borehole logging showed jaggy borehole walls and groundwater flow occurring through five discrete fracture zones at different depths. These fracture zones were observed between 96.4 and 231.9 feet bgs. The observed fractures in

these different zones also appeared to be hydraulically connected. The presence of unstable boreholes, the occurrence of rounded gravel and cobbles, and the observation of discrete fracture zones with hydraulic interconnections suggest a complex and interconnected network of fractures within the bedrock formation. These fractures serve as preferential pathways for groundwater flow, allowing water to move through the bedrock aquifer. Understanding the distribution and connectivity of these fractures is crucial for assessing the movement and availability of groundwater in the karst system.

7.2.4 Large Variation in Aquifer Properties

The specific capacity, which is the yield of a well per unit of drawdown, varied across different wells and zones at the site. The range of specific capacity values observed was significant, ranging from 0.2 to 18.6 gallons per minute per foot. For example, FTMW-16 had the lowest specific capacity compared to the other wells, indicating a relatively lower yield per unit of drawdown. On the other hand, FTMW-14 exhibited the highest specific capacity, indicating a higher yield per unit of drawdown. At FTMW-13, the top zone demonstrated the highest specific capacity, suggesting a relatively higher yield per unit of drawdown in this zone. In contrast, the middle zone exhibited the lowest specific capacity, indicating a lower yield per unit of drawdown in that particular zone. This variation in specific capacity across different zones within the same well suggests heterogeneity in the hydraulic properties of the formation. Similarly, the specific capacity varied at the five zones of FTMW-19. The top zone had the highest specific capacity, indicating a higher yield per unit of drawdown, while the bottom zone showed a lower specific capacity, suggesting a relatively lower yield per unit of drawdown in that zone.

The calculated hydraulic conductivity, which represents the ability of the formation to transmit water, also varied significantly across the site. The range of hydraulic conductivity values spanned three orders of magnitude, with an average value of 17 feet per day. At FTMW-16, despite encountering a clay-filled cavity, the formation intercepted by the well exhibited very low hydraulic conductivity. The borehole could not produce enough water for a meaningful packer test, indicating limited water flow. The calculated hydraulic conductivity for this formation was 0.1 feet per day, although it is noted that this value may be an overestimate. In contrast, at FTMW-14, the presence of a paleochannel or a conduit in the formation resulted in a highly conductive formation, with a calculated hydraulic conductivity of 80 feet per day. This indicates that water can flow very easily through this formation. The hydraulic conductivity values obtained at FTMW-13 indicated vertical heterogeneity in the formation. The top zone had the highest conductivity, suggesting that water can flow most easily through this portion of the formation. Conversely, the middle zone had the lowest conductivity, indicating more restricted or limited water flow through that zone. Similarly, the purging data collected at the five zones of FTMW-19 exhibited a similar trend, with the top zone demonstrating the greatest hydraulic conductivity.

As the depth increased from the top zone to the bottom zone, the hydraulic conductivity progressively decreased. These variations in specific capacity and hydraulic conductivity indicate the heterogeneity and complexity of the subsurface hydrogeological conditions at the site. Understanding these variations is crucial for effective groundwater management and resource evaluation.

7.3 Extent of Contamination

The extent of pollution is represented by the concentrations of the COPCs based on data collected during a certain period. The extents of TCE, cis-DCE and VC were determined based on data collected in November 2013.

7.3.1 Extent of Contamination in the Overburden

Figures 7.10, 7.11 and 7.12 show plumes of TCE, cis-DCE, and VC, respectively. Two TCE plumes were observed in the overburden aquifer. The screening level for TCE is 5 micrograms/liter (μg/L), which defines the lateral extent of the plume. The larger plume, which has an elongated shape, exhibits the highest concentration of 98 μg/L at FTMW-01, near the suspected source area of contamination. This plume spans approximately 100 feet between FTMW-06 and FTMW-10 in the northwest-southeast direction. On the contrary, the smaller plume is located around FTMW-15. Its presence may be attributed to the interaction between contaminant exchanges occurring between the bedrock aquifer and the overburden aquifer at the cutter.

The cis-DCE plume (Fig. 7.11) shows a general shape similar to the shape of the TCE plume. However, the highest cis-DCE concentration of 690 μg/L was detected at further downgradient FTMW-08D, followed by FTMW-01 with a concentration of 100 μg/L. The project screening level for cis-DCE is 70 μg/L, which defines the lateral extent of the plume. At FTMW-09, the cis-DCE concentration was 26 μg/L and at FTMW-15 the cis-DCE concentration was 29 μg/L.

The VC plume (Fig. 7.12) is much smaller than the TCE and cis-DCE groundwater plumes. It has a primarily circular shape. The highest concentration of VC, 430 μg/L, was detected at FTMW-08D, followed by 110 μg/L at FTMW-08. The VC concentration was shown to decrease quickly because the samples at monitoring wells FTMW-06 to the west, FTMW-04 to the north, and FTMW-10/FTMW-15 to the south did not show any detection of VC. The project screening level for VC is 2 μg/L, which defines the lateral extent of the plume. VC was detected in a concentration of 5 μg/L at FTMW-01.

The significant variation in overburden thickness at the site leads to a wide range of depths in the monitoring intervals, making it challenging to define the vertical extent of contamination with a single continuous contour line. However, by analyzing the data from different monitoring wells, some insights can be gained regarding the

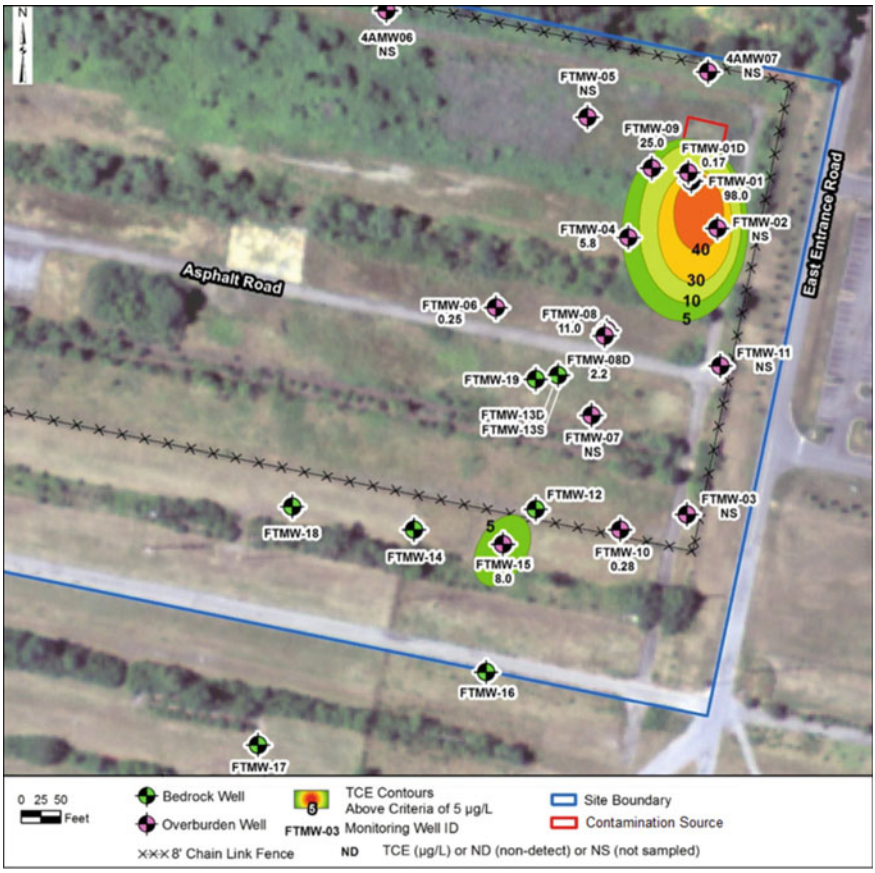

Fig. 7.10 Lateral extent of TCE plume in overburden

vertical extent of the contamination plume. In Fig. 7.13, the vertical profile of the distribution of TCE is illustrated. The deepest monitoring interval at FTMW-15, ranging from 108 to 118 feet bgs, detected TCE at a concentration of 8 µg/L. This suggests that the vertical extent of TCE contamination at FTMW-15 likely extends beyond 118 feet bgs, possibly reaching up to the top of the bedrock.

Overall, the vertical extent of the contamination plume cannot be precisely defined with a single contour line due to the variation in overburden thickness. However, by considering the data from different monitoring wells, it can be inferred that the contamination plume likely extends beyond the depths of the wells and reaches up to the top of the bedrock formation. Further investigation and monitoring are necessary to accurately determine the full vertical extent of the contamination plume.

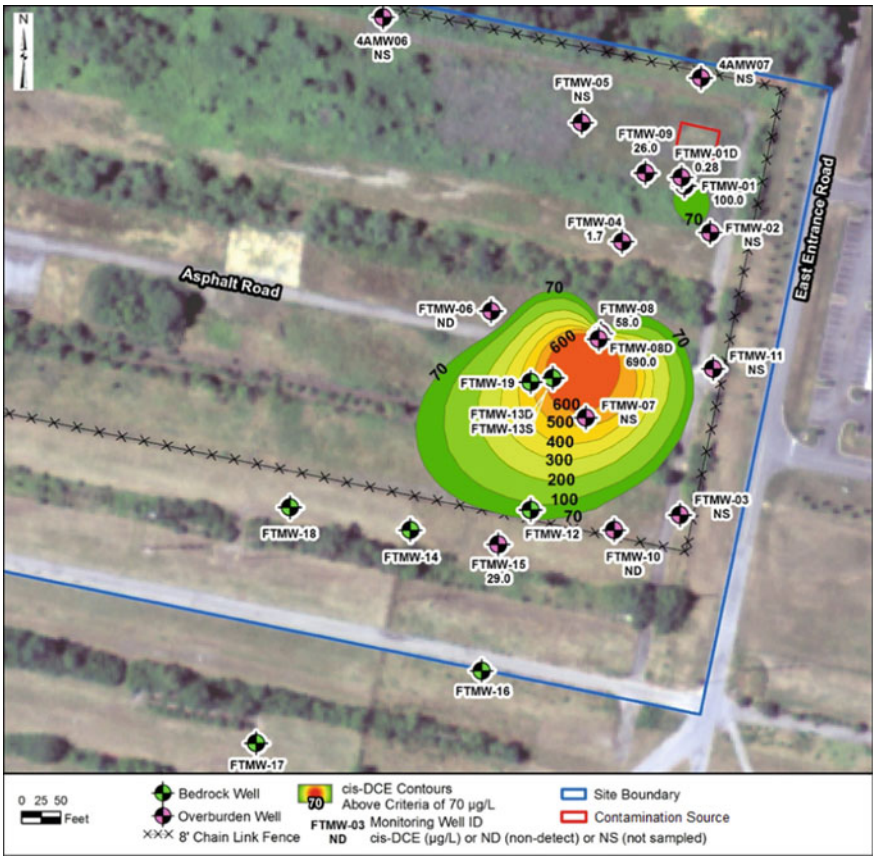

Fig. 7.11 Lateral extent of cis-DCE plume in overburden

7.3.2 Extent of Contamination in the Bedrock Formation

Figure 7.14 provides information on the TCE plume in the bedrock aquifer based on laboratory results collected in November 2013. The lateral extent of the TCE plume in the bedrock aquifer is determined to extend approximately 100 feet from the FTMW-13S/FTMW-13D area in an oval shape. It extends towards the southwest along the pattern of groundwater flow, reaching FTMW-14 and FTMW-18. The TCE concentration of 11 µg/L was detected at their respective depths of FTMW-13D and FTMW-13S. Zone 1 of FTMW-19 exhibits a TCE concentration of 6.6 µg/L.

The vertical extent of TCE contamination in the bedrock aquifer can be determined by examining the observed concentrations in different zones of FTMW-19. Zone 2 recorded an observed TCE concentration of 5.2 µg/L, while Zone 3 had an observed TCE concentration of 4.8 µg/L. Therefore, the vertical extent of contamination in the bedrock aquifer can be inferred to be between the terminus of Zone 2 in FTMW-19 at a depth of 131 feet bgs and the top of Zone 3 at a depth of 138 feet bgs. This

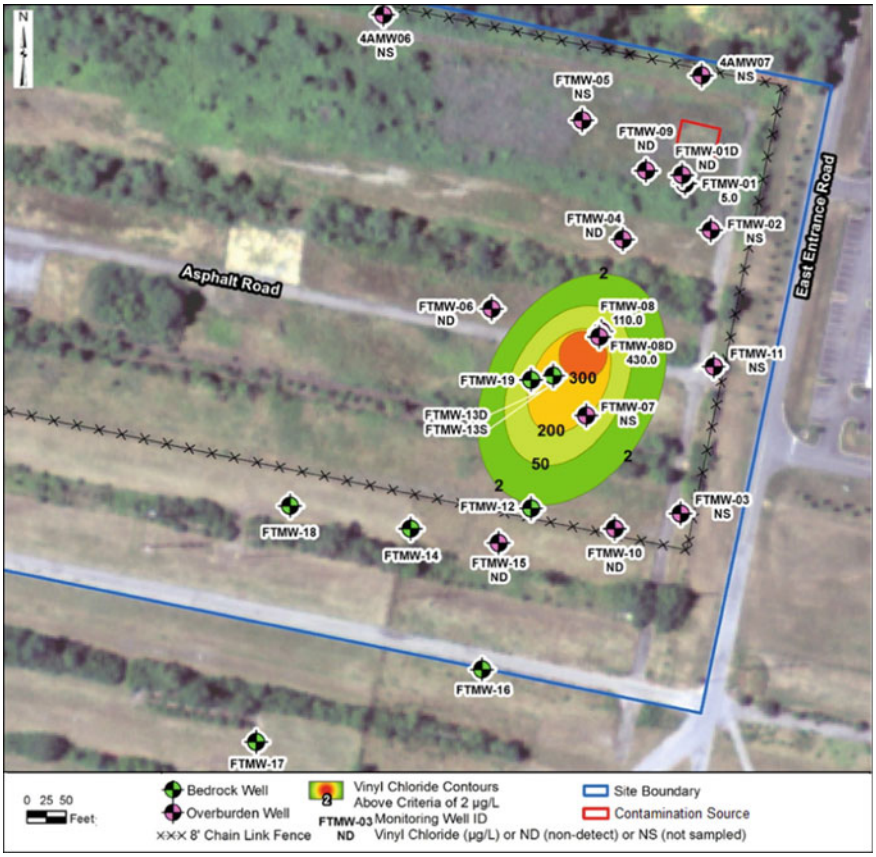

Fig. 7.12 Lateral extent of VC plume in overburden

represents the range of depths where TCE contamination is present in the bedrock aquifer. Figure 7.13 provides a graphical representation of the vertical extent of the TCE plume in the bedrock aquifer.

7.4 Fate and Transport Mechanisms of Chlorinated Hydrocarbon Contaminants

7.4.1 Dense Non-aqueous Phase Liquid Transport

DNAPLs (Dense Non-Aqueous Phase Liquids) are substances that are immiscible with water and have a higher specific gravity compared to water. They include primary halogenated solvents such as TCE, cis-DCE, and VC, as well as their associated

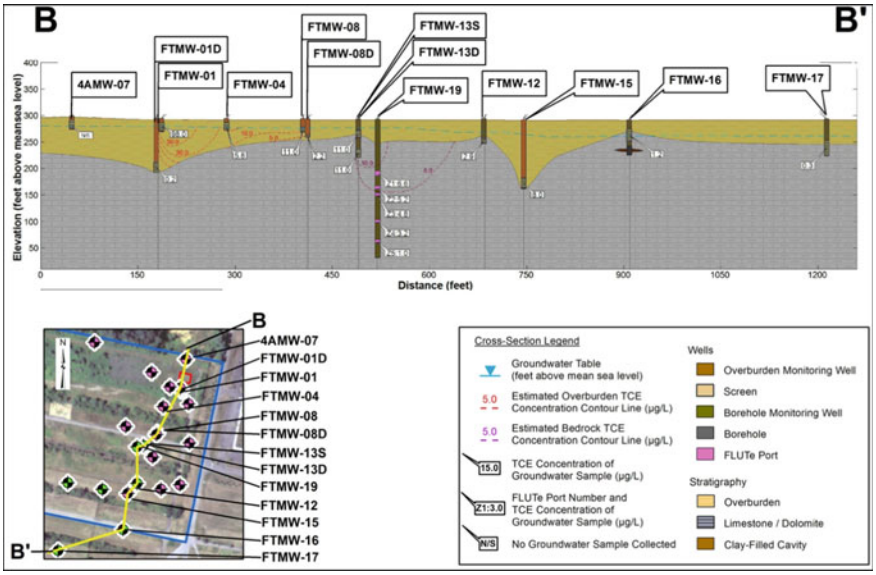

Fig. 7.13 Vertical cross-section of TCE plume in overburden and bedrock

daughter products. The transport of DNAPLs is heavily influenced by the geologic characteristics of the release site (Fig. 7.15). When DNAPLs are released into the subsurface soil in source areas, they typically move vertically downward through the unsaturated zone. However, the separate liquid phase can also move horizontally, depending on variations in soil water content, texture, and structure along the vertical profile. As the DNAPL release approaches the upper region of the capillary fringe (the saturated zone above the water table where water is retained under capillary forces), it begins to spread laterally. This lateral spreading occurs because displacing water from the water-filled voids in the saturated zone becomes more challenging. If enough DNAPL accumulates at the water table, it will enter the saturated zone. Within the saturated soil column, the DNAPL will continue to move downward, potentially being redirected horizontally in response to changes in soil texture. In cases where vertical erosion channels exist in the regolith (loose, fragmented material above bedrock), the DNAPL can migrate rapidly downward, following these channels. When the DNAPL encounters the top of the bedrock or a finer-textured soil layer like clay or silt beneath the upper soil or fill, it may spread out and create a zone of continuously DNAPL-saturated soil. In this zone, most of the water has been displaced by the DNAPL accumulation, forming a "pool" or DNAPL accumulation zone.

In the epikarst layer, the interface between the pinnacled soil and the underlying bedrock plays a significant role in the lateral migration of DNAPL. The DNAPL can accumulate in closed depressions on the bedrock surface or be directed along the relatively impermeable interface, further into the karstified aquifer. The DNAPL then moves through vertical and lateral solution channels, which can be open (filled

Fig. 7.14 Lateral extent of TCE plume in bedrock

with water) or filled with water-saturated residuum and sediment such as sand, silt, clay, gravels, and rock fragments. The movement of DNAPL in open voids is largely unimpeded by capillary forces due to the size of the openings. The primary driving forces for the downward transport are the DNAPL's higher specific gravity compared to water and its immiscibility with water. In contrast, the movement of DNAPL into and through granular residuum is strongly influenced by the size and geometry of the pores and pore throats in that material. DNAPL accumulation zones in open voids can contain separate liquid phase "pools," while the amount of DNAPL per unit volume in accumulation zones within residuum is limited by the porosity of the residuum itself. DNAPL can also migrate vertically and laterally into water-filled discontinuities such as joints, bedding-plane partings, and fractures in the bedrock, which are not enhanced by solution processes. The ease with which DNAPL penetrates such discontinuities is primarily determined by the aperture (size) of the parting in the rock, similar to how it is influenced by the geometry of pore throats in granular soils.

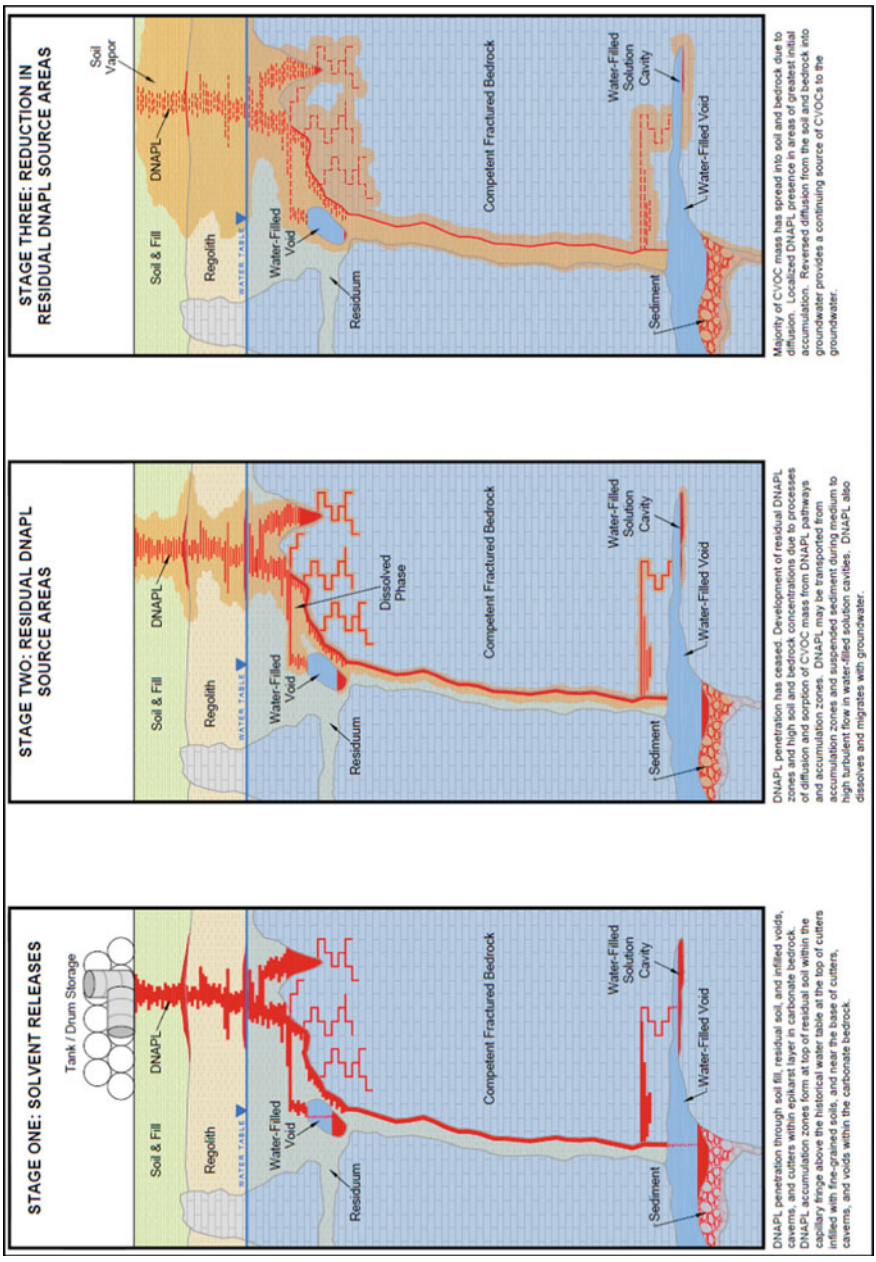

Fig. 7.15 Conceptual models of DNAPL fate and transport in a karst aquifer

In karst aquifers, there is a unique mode of DNAPL transport known as bulk transport. This involves the movement of DNAPL in water flowing at high velocities through open voids. It can occur in sediment-free sections of solution cavities during periods of increased flow when water passes over a DNAPL accumulation zone and picks up droplets of the free DNAPL. Similarly, during open channel flow, sediment particles can be entrained along with DNAPL that may have penetrated into the porous residuum or sediment layer at the bottom of the channel.

7.4.2 Aqueous Phase Transport

Once a DNAPL release reaches equilibrium in the subsurface, where separate phase transport is no longer significant except for entrainment in high-velocity open-channel flow, the mass of DNAPL decreases gradually through two main mechanisms: dissolution in pore water in the vadose zone and groundwater in the saturated zone, and evaporation to the soil vapor in the vadose zone. The dissolution of DNAPL in pore water and groundwater leads to the formation of an aqueous (dissolved) phase of the chlorinated volatile organic compounds (CVOCs). This dissolved phase typically extends along the entire pathway of DNAPL migration. In the area directly affected by the DNAPL release (known as the source area), the concentrations of the dissolved CVOCs near the water-DNAPL interface will approach the solubility of the CVOCs. Figure 7.16 provides an overview of the fate and transport mechanisms for dissolved phase contaminants, illustrating the processes involved in the dissolution and subsequent transport of CVOCs in the subsurface.

Once DNAPL comes into contact with pore water and gravitational water in the vadose zone, as well as groundwater in the saturated zone, an aqueous phase of the CVOCs develops through direct dissolution from the DNAPL (Groundwater Sciences Corporation 2011). The dissolved CVOCs can be transported through the subsurface by two main mechanisms: lateral or vertical advection and diffusion. Aqueous phase advective transport is responsible for the movement of dissolved CVOCs over relatively large distances, from the source area into the plume. This occurs when the groundwater flow carries the dissolved CVOCs along with it. Lateral advection refers to the horizontal movement of the dissolved CVOCs, while vertical advection refers to their vertical movement. Aqueous diffusion, on the other hand, accounts for the movement of dissolved CVOCs over comparatively short distances. This process involves the movement of CVOCs from either the source area or the plume into the pores of the surrounding aquifer material through which advective transport is not occurring on a significant scale. Diffusion occurs due to concentration gradients, with CVOCs moving from areas of higher concentration to areas of lower concentration. These mechanisms of advection and diffusion play a crucial role in the transport of dissolved CVOCs in the subsurface, influencing the spread and migration of contaminants away from the source area and the overall shape and extent of the plume.

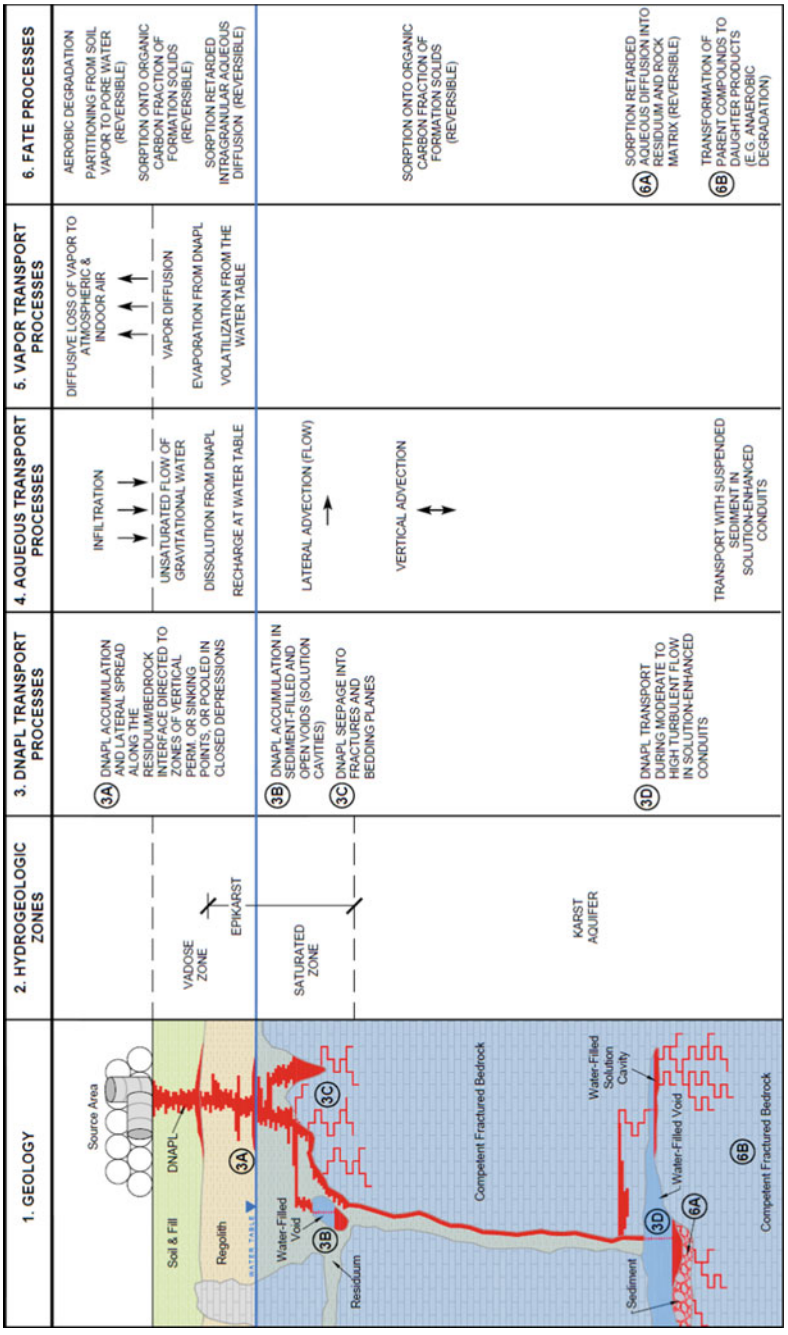

Fig. 7.16 Overview of fate and transport mechanisms for dissolved CVOCs

Aqueous phase advective transport: Aqueous phase advective transport is indeed a crucial process that leads to the formation of a plume consisting of dissolved CVOCs. This plume extends from the source area and can reach a point of discharge, such as surface water bodies or extraction wells. The movement of water from natural sources, including recharge from precipitation infiltration at the ground surface and upgradient groundwater flow, plays a significant role in this process. In the vadose zone (the unsaturated zone above the water table), water infiltrates and moves downward as gravitational pore water, draining freely towards the water table. Within a DNAPL source zone, this gravitational water can directly dissolve soluble compounds from the separate phase liquid associated with the DNAPL source in the vadose zone. The dissolved mass is then transported downward into the saturated zone (the region below the water table). Upgradient groundwater flow entering a specific area can be either uncontaminated if it has not been affected by a source or it can contain dissolved CVOCs. The presence of dissolved CVOCs in the upgradient groundwater can occur due to contact with an upgradient DNAPL source in the saturated zone or through mixing with contaminated recharge from an upgradient location. Recharge into the aquifer at the site serves multiple purposes. It provides the driving force for groundwater flow and the advective transport of CVOCs, allowing the dissolved contaminants to move through the subsurface. Additionally, recharge contributes to the dilution of CVOC concentrations over time, especially after the removal of the DNAPL source. As the diluted groundwater flows through the aquifer, it helps to attenuate and reduce the concentrations of CVOCs in the plume. Furthermore, there is the potential for vertical advection of groundwater downward into and through highly permeable fractured and solution-enhanced zones in the carbonate bedrock. This vertical advection can further influence the transport of CVOCs in the subsurface, allowing the dissolved contaminants to migrate vertically and potentially impact deeper aquifers or discharge points.

Aqueous phase dispersion: Hydrodynamic dispersion involves the mixing of a solute in both horizontal and vertical directions as it is transported through a medium. This process leads to the blending of neighboring aqueous solutions or the displacement of such solutions. In order to estimate the longitudinal dispersivity, researchers have collected data from various sources. A study conducted by Lallemand-Barres and Peaudecerf (1978) presented a graph that suggests the field-scale longitudinal dispersivity is approximately one-tenth of the characteristic length scale. Expanding on this research, Neuman (1990) further investigated the topic and proposed a universal scaling rule. Neuman established a correlation between longitudinal dispersivity and the investigation scales in different porous media, considering diverse conditions of groundwater flow and solute transport. The data utilized in Neuman's study were derived from both laboratory experiments and field-scale investigations. The most general equation derived by Neuman is Eq. 7.2:

$$\alpha_L = 0.0175 L_s^{1.46} \tag{7.2}$$

where, α_L is the longitudinal dispersivity and L_s is the characteristic scale length.

The characteristic length is a unique parameter specific to each site, which relies on the distribution of hydraulic conductivity within a particular aquifer or groundwater flow system. It is defined as the minimum length of groundwater flowpaths where a migrating solute encounters all possible variations in hydraulic conductivity. The characteristic length is influenced by the heterogeneity and anisotropy of the aquifer.

In a study conducted by Gelhar et al. (1992), scatter diagrams similar to those presented by Neuman (1990) were published. These diagrams compared the longitudinal dispersivity to the observation scale. Within a given scale, the values of longitudinal dispersivity varied across 2–3 orders of magnitude. The authors emphasized that the lower end of this range was considered the most reliable. For instance, projecting a measurement scale of 250 feet to the approximate center of the scatter data corresponded to a longitudinal dispersivity of approximately 32 feet (10 m). Furthermore, Gelhar et al. (1992) highlighted that vertical dispersivities are typically one order of magnitude smaller than transverse dispersivities, and transverse dispersivities are typically one order of magnitude smaller than longitudinal dispersivities. This indicates significant differences in dispersivity values depending on the direction of dispersion (longitudinal, transverse, or vertical).

Aqueous phase diffusion: In addition to groundwater flow, dissolved chlorinated volatile organic compounds (CVOCs) can also be transported through aqueous diffusion. This diffusion process occurs in the groundwater present in the pores between individual soil particles in residuum or sediments, as well as in the primary porosity of bedrock, in response to a concentration gradient of the chemicals. Aqueous diffusion can occur both in the area where dense non-aqueous phase liquid (DNAPL) is present and in the plume that emanates from it. Research conducted at the University of Waterloo by Plett (2006) and Kennel (2008) has demonstrated that DNAPL held in bedrock fractures by capillary forces can gradually diffuse into the pore water contained within the rock, depending on the characteristics of the surrounding rock matrix. This phenomenon is known as "matrix diffusion." As a result, the DNAPL in individual fractures can be completely eliminated, and the mass of CVOCs that was previously present as DNAPL becomes dissolved in the aqueous phase. This leads to high-concentration dissolved CVOCs in the pore water within the rock matrix adjacent to the fracture that previously contained the DNAPL.

Matrix diffusion can occur not only in the solid rock surrounding fractures and open voids but also in porous granular materials such as residuum and sediment that fill voids in carbonate bedrock. When DNAPL comes into contact with these materials, matrix diffusion can take place. The process of matrix diffusion in residuum and sediment is typically a two-stage process. Initially, the dissolved CVOCs diffuse into the intergranular pores, which are the water-filled spaces between individual soil grains. As the concentrations of CVOCs build up within these intergranular pores, diffusion then occurs into the intragranular pores. These intragranular pores are associated with the primary porosity of individual soil grains, which are eroded fragments of sedimentary rocks. This two-stage diffusion process continues as long as there is a concentration gradient between the groundwater in contact with the DNAPL and the aqueous concentrations within the intergranular and intragranular

pore water. DNAPL releases can persist for several decades without remediation, and during this time, substantial mass transfer can occur from the separate phase (DNAPL) to the aqueous phase through aqueous diffusion. As a result, a significant percentage of the originally released mass can be transferred to the aqueous phase, which becomes a repository for the dissolved CVOCs in the environment.

Estimating the amount of DNAPL released to the environment and determining the extent of matrix diffusion can be challenging. However, when separate phase DNAPL encounters a geological medium with interconnected pores containing clean pore water, a concentration gradient is established, leading to the diffusion of mass from the dissolving DNAPL into the neighboring pore water.

Matrix diffusion can also take place within the plume area. When advective transport takes place in fractures and solution conduits, a plume area is generated. Within this plume area, matrix diffusion is triggered by the significant chemical gradient between the open conduits in the carbonate aquifer, where preferential advective transport of dissolved CVOCs occurs, and the surrounding solid rock, residuum, or sediment. These geological materials typically have lower hydraulic conductivity and do not serve as the primary pathways for plume migration. As such, groundwater flowing through fractures and carrying dissolved CVOCs comes into direct contact with groundwater present in the pores of the adjacent rock matrix, residuum, and sediment. This contact creates a chemical diffusion gradient, causing the CVOCs to diffuse from the water within the fractures to the water in these pores of the surrounding geological materials.

7.4.3 Vapor Phase Transport Processes

The development of the vapor phase in the subsurface is influenced by two mechanisms: direct evaporation of chlorinated volatile organic compounds (CVOCs) from residual DNAPL in the vadose zone and volatilization of CVOCs from groundwater at the water table.

Evaporation from residual DNAPL in the vadose zone is predominantly controlled by the vapor pressure exhibited by each specific compound. In close proximity to the DNAPL source, this phenomenon typically gives rise to vapor phase concentrations that closely approach the saturation concentration of each substance in the surrounding air. The vapor pressure of a compound determines its tendency to evaporate, with higher vapor pressures leading to more significant evaporation. On the contrary, volatilization of CVOCs from the water table is influenced by the concentration of each compound in the groundwater and its Henry's Law constant. Henry's Law constant relates to the ability of a compound to partition between the water phase and the vapor phase. Generally, direct evaporation from residual DNAPL is expected to produce higher vapor phase concentrations compared to volatilization from groundwater. This is mainly because these substances have relatively low solubility in groundwater, meaning they are less likely to be present in high concentrations in the water phase.

Once in the vapor phase, the primary mechanism of transport for chlorinated volatile organic compounds (CVOCs) is vapor diffusion. Vapor diffusion takes place as a response to the concentration gradient between relatively high vapor concentrations in the soil air and negligible concentrations of these substances in the atmospheric air. Consequently, vapor diffusion primarily facilitates the upward movement of CVOCs (Chlorinated Volatile Organic Compounds) from DNAPL source zones in the vadose zone and from dissolved contaminants at the water table, directing them towards the ground surface. This process results in the loss of VOC mass through diffusion to the atmosphere.

In addition to vapor diffusion, vapor transport can also occur through advection. Advection refers to the movement of vapors due to the bulk flow of air. For example, in buildings constructed over a source or plume, vapor transport may happen across the concrete slab in response to a pressure difference across the slab. This can result in the movement of CVOC vapors along with the air flow. Another form of advective transport is known as "barometric pumping." Barometric pumping occurs when changes in atmospheric pressure create a pressure gradient between the soil air and the atmospheric air. This pressure gradient can cause the movement of a volume of soil air containing CVOC vapors, in addition to the individual VOC molecules, as opposed to just the diffusion of VOCs.

7.4.4 CVOC Fate Processes

Fate processes lead to the depletion of chlorinated volatile organic compounds (CVOCs) through degradation, temporary storage via sorption, or transformation in both the saturated and unsaturated zones.

Partitioning from soil vapor to pore water in the vadose zone: Within the vadose zone, a fraction of the CVOCs found in the soil vapor undergoes partitioning, distributing into the pore water that envelops the individual soil grains. Similar to the volatilization process occurring at the water table, which contributes to the presence of CVOCs in the vapor phase, this partitioning mechanism from the vapor phase to the pore water is influenced by the unique Henry's Law constant associated with each specific CVOC.

Sorption on formation solids: In both the saturated and unsaturated zones, sorption of VOCs onto the organic carbon fraction of formation solids can take place. In the zone of saturation, this sorption takes place through direct partitioning from the aqueous phase to the solid phase, irrespective of the presence of DNAPLs. In the vadose zone, the sorption process can occur directly from the aqueous phase to the solid phase if DNAPLs are in contact with the pore water. However, in the absence of DNAPLs, this sorption process follows a two-step pathway. Firstly, there is partitioning from the soil vapor to the pore water, as discussed earlier. Subsequently, the VOCs partition from the pore water to the solid phase.

Limited information is available regarding the organic carbon content of carbonate at the site. However, studies conducted at the University of Waterloo by Plett (2006) and Kennel (2008) have provided some insights into the fractional mass of organic carbon (foc) in the matrix of the Silurian dolostone, which was the focus of their research. Plett (2006) reported a range of foc values in dolostone of 0.003–0.125%, with an average of 0.017%. These results suggest a relatively low sorption potential for the dolostone. Similarly, Kennel (2008) provided data on various components of the dolostone bedrock. For the dolostone matrix, Kennel reported values ranging from 0.01 to 0.10%, with an average of 0.02%, which closely aligns with Plett's findings. However, Kennel's data revealed significant variations in sorption potential depending on the specific location within the dolostone. In a single sample from a stylolite layer, he reported a foc value of 3.5%, indicating a higher sorption potential in that particular layer. Notably, for 15 samples taken from fracture surfaces, Kennel reported a range of 0.08–6.36%, with an average of 2.31%. These results indicate a substantial sorption potential on fracture surfaces within the dolostone. In fact, the data suggest that the sorption potential on the surface of fractures is more than 100 times greater than that of the dolostone rock matrix. Sorption is quantified as a coefficient of retardation (R), which can be expressed as a function of the distribution of an organic compound between the aquifer matrix and the aqueous phase (Eq. 7.3):

$$R = 1 + \rho K_d / n \tag{7.3}$$

where R is the coefficient of retardation; ρ is the bulk density of the aquifer matrix. K_d is the distribution coefficient, as defined by sorbed concentration divided by dissolved concentration. The porosity is represented by n.

The distribution coefficient (K_d) can also be expressed as Eq. 7.4:

$$K_d = K_{oc} f_{oc} \tag{7.4}$$

where K_{oc} is the soil sorption coefficient to organic carbon and f_{oc} is the fractional mass of organic carbon in the matrix.

In addition to sorption onto organic carbon, Loop and White (2001) have reported that CVOCs can also adsorb to the surface of metal oxide coatings. These coatings are predominantly found in the quarzitic sandstones of the Antietam Formation but can also be present in the carbonate bedrock aquifer. Similar to sorption onto carbon, this adsorption process results in the removal of mass from the CVOCs present in groundwater, thus influencing their transport behavior. The adsorption onto metal oxide coatings provides an additional mechanism for the retention and attenuation of CVOCs in the subsurface. Assessing the significance of this mechanism for the study site requires site-specific determinations of fractional mass of organic carbon (f_{oc}) for granular materials such as residuum and sediment, as well as for the rock matrix and fracture surfaces, as performed in the studies conducted at the University of Waterloo (Plett 2006; Kennel 2008). Without such data, it is challenging to evaluate the importance of adsorption onto metal oxide coatings at the site. However,

if the site conditions are similar to those described in the previous studies, sorption onto fracture surfaces can remove a portion of the CVOC mass dissolved in groundwater as it flows through those fractures. This sorption process can contribute to secondary sourcing once CVOC concentrations start to decline and desorption occurs. Additionally, if the residuum and/or sediments at the site have a significant organic carbon fraction (foc), sorption and desorption processes associated with these materials can also be substantial, particularly if they result in sorption-retarded reverse diffusion. In such cases, CVOCs that have sorbed onto these materials may be gradually released back into the groundwater over time, potentially prolonging the persistence of contaminants in the subsurface environment. These sorption and desorption processes can have important implications for the fate and transport of CVOCs in the subsurface, as they can influence the overall mass balance and the long-term behavior of contaminants in the aquifer.

7.4.5 Bio-reductive Dechlorination of Organic Compounds

Under anaerobic conditions, the chlorinated solvents frequently detected in groundwater at contaminated sites have the potential to undergo biotic reductive degradation. This natural process involves the activity of specific microorganisms capable of utilizing the chlorinated solvents as electron acceptors during their metabolic activities. As a consequence, the chlorinated solvents undergo a series of sequential dechlorination reactions, leading to the formation of less chlorinated compounds. This process is facilitated by natural bacteria that possess the ability to carry out reductive dechlorination. Figure 7.17 summarizes the degradation pathways of CVOCs, starting from PCE. The pathways highlighted in red are the most commonly accepted degradation processes, although the actual degradation pathways are site-specific. Reductive dechlorination is often the dominant process for the more chlorinated CVOCs. PCE, with its four chlorine atoms, readily undergoes reductive dechlorination to TCE under anaerobic conditions. Furthermore, the tendency of chlorinated ethenes to undergo reductive dechlorination decreases as the number of chlorine substituents decreases.

In many water bearing formations, the rate of each step in the reductive dechlorination process tends to slow down as the transformation progresses. Consequently, the concentrations of later degradation products, such as cis-DCE or VC, may appear to increase relative to the concentrations of the parent solvents. This observation is commonly made when geochemical conditions continue to favor reductive dechlorination. In certain cases, the relative concentrations of degradation products may even increase with increasing distance from the source zone. This phenomenon occurs when the geochemical conditions required for reductive dechlorination remain favorable over a greater distance from the original source. Furthermore, the relative concentrations of transformation products can also exhibit an increase over time at a specific location. This is because the biogeochemical conditions may become more favorable for reductive dechlorination as time progresses.

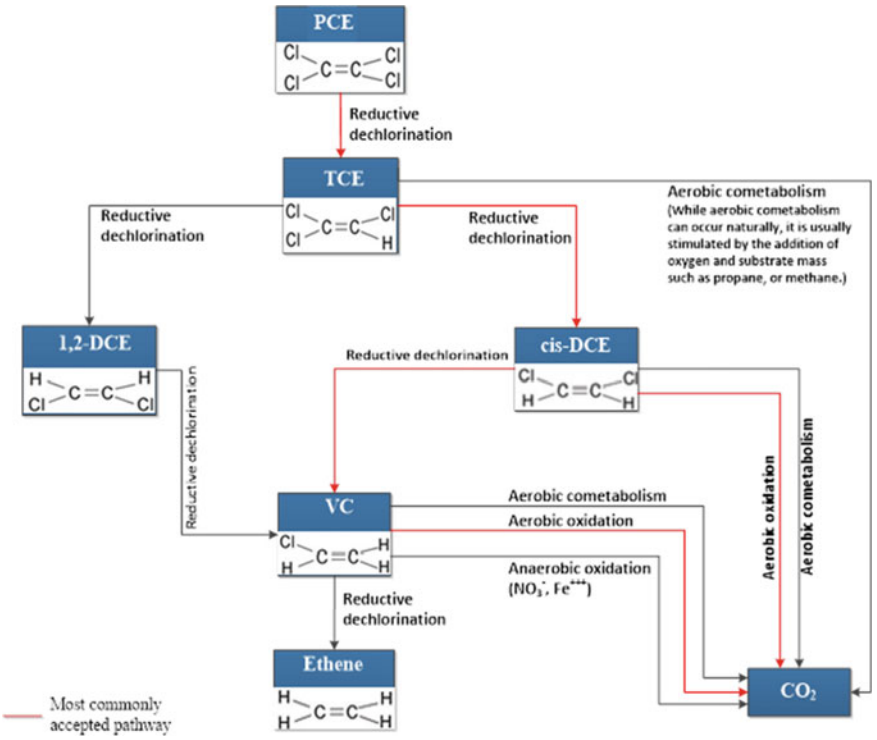

Fig. 7.17 Summary of microbial biodegradation pathways

These transformations typically take place in source areas where chlorinated volatile organic compounds (CVOCs) were co-disposed with other organic compounds, such as petroleum products. The biodegradation of these co-disposed substances often generates geochemical conditions, such as sulfate-reducing or methanogenic conditions, that are conducive to the reductive dechlorination of CVOCs. Rate of degradation is commonly expressed in degradation coefficient. The degradation coefficients for TCE, cis-DCE, and VC are shown in Table 7.8. The half-lives of the contaminants, in years, can be calculated by dividing 0.7 by the degradation coefficient.

Table 7.8 Select chemical properties of CVOCs

Compound	K_{oc} (l/kg)	Solubility (mg/l)	Degradation coefficient (1/year)	Half-life (years)
Trichloroethene	93	1100	0.02	35
cis-1,2-dichloroethene	49	3500	0.01	70
Vinyl chloride	10	2700	0.09	7.8

The degradation of organic compounds takes place through electron transfers between a donor and an acceptor, typically in an environment with reduced oxygen levels. These chemical reactions, known as biologically mediated redox reactions, are facilitated by naturally occurring microorganisms. Microbial degradation is most efficient when the concentrations of organic constituents are at low to moderate levels. Microorganism populations that are capable of effectively breaking down organic compounds thrive within a pH range of 5–9. As organic compounds undergo oxidation, carbon dioxide is produced, leading to the formation of carbonic acid in groundwater. This process effectively lowers the pH of the groundwater. The redox potential, which reflects the oxygenation potential of a groundwater environment, is typically above 50 millivolts (mV) in aerobic environments, accompanied by dissolved oxygen (DO) concentrations greater than 0.8 mg/L.

Microbial degradation of organic compounds can lead to the transition from an aerobic environment to an anaerobic one as electron acceptors are progressively depleted (Environmental Security Technology Certification Program 2011). Initially, when organic compounds are introduced, microbial populations consume the available oxygen in the environment. As oxygen becomes limited, microorganisms sequentially utilize alternative electron acceptors for respiration, such as nitrate, manganese oxide, ferrous oxide, and sulfate.

In the context of organic compound plumes, aerobic degradation typically occurs at the outer edges or limits of the plume where oxygen is still available. As the plume progresses inward, towards the center, the oxygen concentration decreases, creating an anaerobic environment. Within the anaerobic zone of the plume, microorganisms rely on alternative electron acceptors for their metabolic activities. Different zones of reduction, supported by specific electron acceptors, can be observed within contaminant plumes. For example, the presence of ferrous iron and manganese oxide can facilitate anaerobic degradation processes in certain zones. These compounds serve as electron acceptors for microorganisms, enabling their metabolic activities in the absence of oxygen.

7.4.6 Abiotic Degradation

Dechlorination without microbes was recognized in late 1980s. Research has demonstrated that chemically precipitated ferrous iron can serve as an active reductant for CVOCs. Additionally, the development of zero valent iron (ZVI) technology has contributed to the growing interest in abiotic degradation of contaminants. In 2002, a study by Ferrey and Wilson (2002) showed that a plume of cis-DCE, a CVOC, was abiotically degraded by magnetite, a mixed ferrous and ferric oxide. The degradation rates observed with magnetite were comparable to biological processes, indicating the effectiveness of abiotic degradation for CVOCs. In this context, ferrous iron plays a similar role to microbes in reductive dechlorination, acting as a reductant for CVOCs.

Figure 7.18 illustrates the common abiotic degradation pathways of CVOCs. The primary abiotic degradation mechanism for CVOCs is reductive elimination. This process involves a two-electron transfer to the target molecule, leading to the elimination of two chlorine atoms. The result is the formation of relatively benign degradation products. For instance, TCE can undergo dichloroelimination via reductive elimination, forming acetylene as an intermediate product. This reaction involves the removal of two chlorine atoms from TCE, resulting in the transient formation of chloroacetylene. Subsequently, acetylene may undergo further reactions, such as hydrogenation, under specific conditions (Arnold and Roberts 2000).

Hydrogenolysis is a commonly observed mechanism in abiotic degradation processes facilitated by reactive minerals, although its contribution is typically minor compared to reductive elimination. Hydrogenolysis involves the reductive breaking of a carbon-chlorine bond, with hydrogen replacing chlorine and the addition of two electrons to the molecule (Tobiszewski and Namiesnik 2012). Butler and Hayes

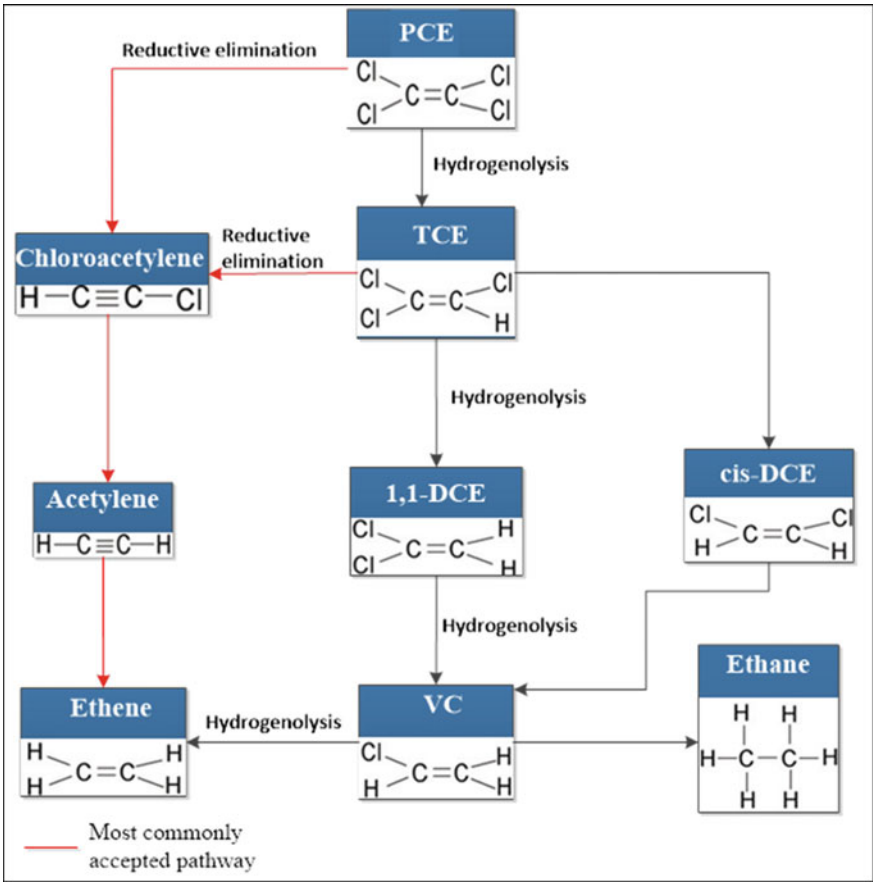

Fig. 7.18 Summary of abiotic biodegradation pathways

(1999) demonstrated that in iron sulfide (FeS) systems at pH 8.3, trichloroethylene (TCE) was transformed to acetylene 11.8 ± 1.1 times faster than to cis-DCE, while tetrachloroethylene (PCE) was transformed to acetylene 8.2 ± 1.8 times faster than to TCE.

Acetylene is the most common degradation product resulting from reductive elimination and is often considered a characteristic product of the abiotic degradation of chlorinated solvents (He et al. 2015). The specific degradation product resulting from the hydrogenolysis pathway depends on the parent compound, with each step sequentially removing one chlorine atom.

Butler and Hayes (1999) proposed that FeS can transform PCE through parallel reaction pathways, leading to the formation of acetylene, TCE, and cis-DCE. Jeong and Hayes (2007) reported that PCE can be transformed to TCE via hydrogenolysis, forming acetylene and 1,1-DCE. Similar mechanisms and degradation products have been observed for the degradation of PCE by pyrite and green rust (Lee and Batchelor 2002).

Likewise, the transformation of TCE by FeS occurs through parallel reaction pathways. TCE can be converted to acetylene through reductive elimination, with chloroacetylene as an intermediate, or via hydrogenolysis to cis-DCE (Butler and Hayes 1999; Jeong and Hayes 2007). Acetylene was identified as the major product in the reductive transformation of TCE by FeS, followed by cis-DCE. Similar degradation mechanisms and product distributions have been observed for TCE degradation by troilite, pyrite, and green rust (Lee and Batchelor 2002).

Regarding the reductive dechlorination of cis-DCE by pyrite, Lee and Batchelor (2002) suggested that the main pathway is reductive elimination. However, cis-DCE does not appear to react with FeS (Jeong and Hayes 2007). The dechlorination of vinyl chloride by pyrite follows a hydrogenolysis pathway, resulting in the production of ethene and ethane, with ethene further reduced to ethane. The major abiotic degradation pathways and products for the degradation of PCE and TCE are similar for minerals such as FeS, magnetite, green rust, and Fe^{2+}-sorbed minerals. Reductive elimination is the primary degradation pathway, with acetylene being the major degradation product.

7.4.7 Aerobic/Anaerobic Oxidation

The primary solvents, PCE and TCE, do not undergo significant biodegradation under oxidizing conditions in groundwater. However, under appropriate conditions, their daughter products, cis-1,2-dichloroethylene (cis-DCE) and vinyl chloride (VC), can undergo degradation through aerobic or anaerobic oxidation processes. These degradation pathways occur without the formation of easily identifiable degradation products. Depending on the depth to the water table, cis-DCE and VC may degrade aerobically in the vadose zone, which reduces their potential impact as concerns for vapor intrusion into occupied structures. Table 7.9 summarizes the various degradation mechanisms of CVOCs. Degradation through either microbial or abiotic process

is a destructive mechanism that leads to reduction in loads of CVOCs in groundwater. The degradation together with the nondestructive natural attenuation mechanisms including sorption, dispersion, and dilution controls fate and transport of CVOCs in many groundwater systems. Complete degradation of CVOCs can result in the transformation of these compounds into environmentally benign substances such as carbon dioxide (CO_2), ethene, and chloride ions. However, it is important to note that some transformation products, like vinyl chloride (VC), can actually increase the toxicity of chlorinated solvents. To comprehensively understand the fate of CVOCs and their degradation, it is crucial to establish a conceptual site model that can be used for contaminant transport modeling, characterizing exposure pathways, and conducting analyses to select appropriate remedial alternatives. The effectiveness of CVOC degradation is highly dependent on the site-specific hydrologic, biologic, and geochemical characteristics of the groundwater system. These factors play a significant role in determining the availability of electron acceptors or donors, the presence of suitable microbial communities, and the overall conditions necessary for degradation processes to occur.

7.4.8 Secondary Sourcing

Figure 7.16 highlights several processes that have been identified as reversible in the context of the topic discussed. These reversible processes include.

Aqueous diffusion refers to the movement of water molecules into the pore spaces of different geological formations, including carbonate rock matrices, residua, and sediments that fill voids within the carbonate rock. This diffusion process occurs in both dense non-aqueous phase liquid (DNAPL) source areas and chlorinated volatile organic compound (CVOC) plume areas. This means that the movement of water into these porous media can occur in both directions, allowing for the exchange of dissolved contaminants.

Partitioning from soil vapor or DNAPL to pore water in the vadose zone. This indicates that contaminants can move between the vapor phase and the water phase in the unsaturated zone. They can either partition from the vapor phase into the pore water or vice versa, depending on the prevailing conditions.

Sorption onto the organic carbon fraction of formation solids and metal oxide coatings in both the saturated and unsaturated zones. This refers to the reversible process of contaminants attaching to the organic carbon present in the solid formations and the coatings of metal oxides. Contaminants can desorb from these surfaces back into the water phase under certain conditions. These processes effectively retain mass within the solid phase of soil and bedrock, with the extent of mass storage and its persistence influenced by various factors. The presence of dense non-aqueous phase liquid (DNAPL) as a primary source of contamination in water and vapor, as well as the existence of groundwater containing constituents at higher concentrations than the original levels, play a crucial role in determining the amount of sorbed and diffused mass.

Table 7.9 Summary of degradation mechanisms of CVOCs

Environment		Mechanism	Processes
Microbial degradation	Anaerobic conditions	Reductive dechlorination	• Microbial reductive dechlorination is a widespread process observed in anaerobic aquifers contaminated with CVOCs) However, the degree of dechlorination can vary significantly from one site to another • The reductive dechlorination process tends to decrease in efficiency as the number of chlorine atoms in the molecule decreases. For example, PCE, which contains four chlorine atoms, readily undergoes reductive dechlorination to form TCE. However, this transformation is less likely to occur in aerobic aquifers where oxygen is present • The reductive dechlorination of TCE to cis-dichloroethene (cis-DCE) occurs under conditions where Fe(III) is being reduced and in more strongly reducing environments • The reductive dechlorination of cis-DCE to vinyl chloride (VC) typically requires the presence of sulfate (SO_4)-reducing conditions, although it can also occur in methanogenic environments • The reductive dechlorination of VC to non-chlorinated ethene is known to be slow and significant only under highly reducing, methanogenic conditions • In groundwater systems, the reductive dechlorination of chloroethene contaminants is often incomplete, leading to the accumulation of cis-DCE and VC as intermediate products • Complete reductive dechlorination to ethene may be possible when dehalococcoides (DHC) microbes are present in substantial numbers in groundwater systems

(continued)

Table 7.9 (continued)

Environment		Mechanism	Processes
		Anaerobic oxidation	• Under anaerobic conditions, the oxidation of cis-DCE and VC can occur if there is a strong oxidant present to drive microbial degradation • Fe(III) oxides are strong oxidants when it is present in groundwater systems. Low but significant VC mineralization has been detected in anaerobic microcosms under ambient Fe(III) conditions • The combination of reductive dechlorination of PCE and TCE in anaerobic conditions, followed by the subsequent anaerobic microbial oxidation of cis-DCE and VC, presents a potential microbial pathway for achieving the complete degradation of CVOCs within groundwater system
	Aerobic conditions	Aerobic oxidation	• The tendency to undergo oxidation increases as the number of chlorine substituents decreases. VC, being the least chlorinated among the CVOCs, exhibits the highest propensity for oxidation • Microbial oxidation of DCE and VC to CO_2 has been observed under aerobic conditions, however, this mechanism is of limited relevance in most groundwater systems • The aerobic biodegradation of CVOCs in groundwater systems is likely restricted to the periphery of the contaminant plume, where the dissolved oxygen (DO) has not been depleted due to microbial respiration

(continued)

Table 7.9 (continued)

Environment		Mechanism	Processes
		Aerobic cometabolism	• Cometabolic oxidation is generally not regarded as a significant mechanism for the biodegradation of CVOCs in groundwater • Aerobic cometabolism requires the presence of oxygen and a primary substrate to initiate the production of a suitable oxygenase • Aerobic microorganisms, including methane, propane, ethene, aromatic compound, ammonium, isoprene, and VC oxidizers, are capable of oxidizing TCE, cis-DCE, and VC to CO_2 without accumulation of toxic intermediates • In aerobic aquifers contaminated with TCE, biodegradation can occur through the activity of methanotrophic microorganisms when an adequate supply of methane is introduced into the subsurface to stimulate and support their activity
Abiotic degradation	Anaerobic conditions	Reductive elimination or dichloroelimination	• Reductive elimination primarily takes place under methanogenic conditions, where the presence of methanogenic microorganisms facilitates the process. However, it can also occur under partially aerobic conditions, although to a lesser extent • Reductive elimination is a chemical process that involves a two-electron transfer to the target molecule, resulting in the elimination of two chlorine atoms • PCE and TCE undergo dichloroelimination, leading to the formation of acetylene through the transient intermediate chloroacetylene. Acetylene can then undergo further reactions, such as hydrogenation, resulting in the formation of ethene and/or ethane • Iron-bearing minerals, such as iron sulfides (pyrite and mackinawite), green rust, iron oxides (magnetite), and iron-bearing clays, play a crucial role in these processes • Reactive iron minerals are commonly found in subsurface environments under conditions characterized by iron reduction and sulfate reduction
	Anaerobic conditions	Hydrogenolysis	• Hydrogenolysis is a reductive reaction that involves the cleavage of a carbon-chlorine bond, resulting in the replacement of chlorine with hydrogen • Sequential hydrogenolysis involves the sequential replacement of chloro-substituents with H from protons, releasing chloride • TCE can undergo sequential hydrogenolysis, forming cis-DCE, followed by VC, and ethene in the presence of iron sulfide and/or zero valent iron (ZVI)

As groundwater concentrations experience significant decreases, a reversal of these processes occurs, commonly referred to as reverse diffusion and desorption. This reversal leads to the release of previously stored mass back into the flowing groundwater within the saturated zone and the gravitational water within the vadose zone. Through desorption and reverse diffusion, the mass, previously held within the solid phase, is reintroduced into the aqueous phase. Since this stored mass can re-enter the aqueous phase, it acts as a secondary source of groundwater contamination, potentially impeding the decline of groundwater concentrations over time. These processes often contribute to the observed tailing effect in groundwater monitoring data at sites undergoing remediation for chlorinated volatile organic compounds (CVOCs).

7.4.9 Evidence of Natural Attenuation

The confirmation of natural attenuation typically involves assessing a series of evidence that supports the overall degradation process. One primary piece of evidence is the evaluation of historical analytical data.

Concentration reduction indicators: The geochemical groundwater data collected from the monitoring wells are the best indicators of biodegradation occurrence. Based on chemographs of CVOCs, results of monitored natural attenuation parameters (e.g., sulfate, nitrate, chloride, iron, etc.) and the presence and distribution of cis-DCE and VC (byproducts of biodegradation of TCE), conditions for natural attenuation can be determined. The presence of VC, in addition to cis-cis-DCE, is a strong indicator of chemical and natural attenuation of the CVOC plumes. Given the correct environmental conditions, over time VC may mineralize into CO_2, H_2O, and a chloride ion in addition to ethene and ethane which readily volatilize into the vadose zone and ultimately the atmosphere. Figure 7.19 shows a pie diagram for TCE, cis-DCE, and VC to demonstrate their relative distributions. The size of the pie indicates the relative magnitude of the total concentration of three chemicals. Because of the heterogeneous nature of the site, a definitive pattern is not obvious. In general, the data show some diminishing levels of TCE downgradient, but also increases in the concentrations of breakdown products (cis-DCE and VC).

The concentration changes tend to be great where the groundwater was firstly contaminated the most. The maximum concentration of cis-DCE was detected in FTMW-08D at 2900 μg/L in October 2008. In a groundwater sample collected in November 2013, the cis-DCE concentration had decreased to 690 μg/L. In FTMW-04, the cis-DCE concentration decreased by a factor of 70 from 2008 to 2013. The greatest decrease was observed in FTMW-08, where the cis-DCE concentration decreased from 2600 μg/L in October 2008 to 58 μg/L in November 2013. The most obvious TCE concentration change occurred in FTMW-04, decreasing from 180 μg/L in June 2008 to 5.8 μg/L in November 2013. The maximum TCE concentration decrease took place in FTMW-01 from 850 μg/L in June 2008 to

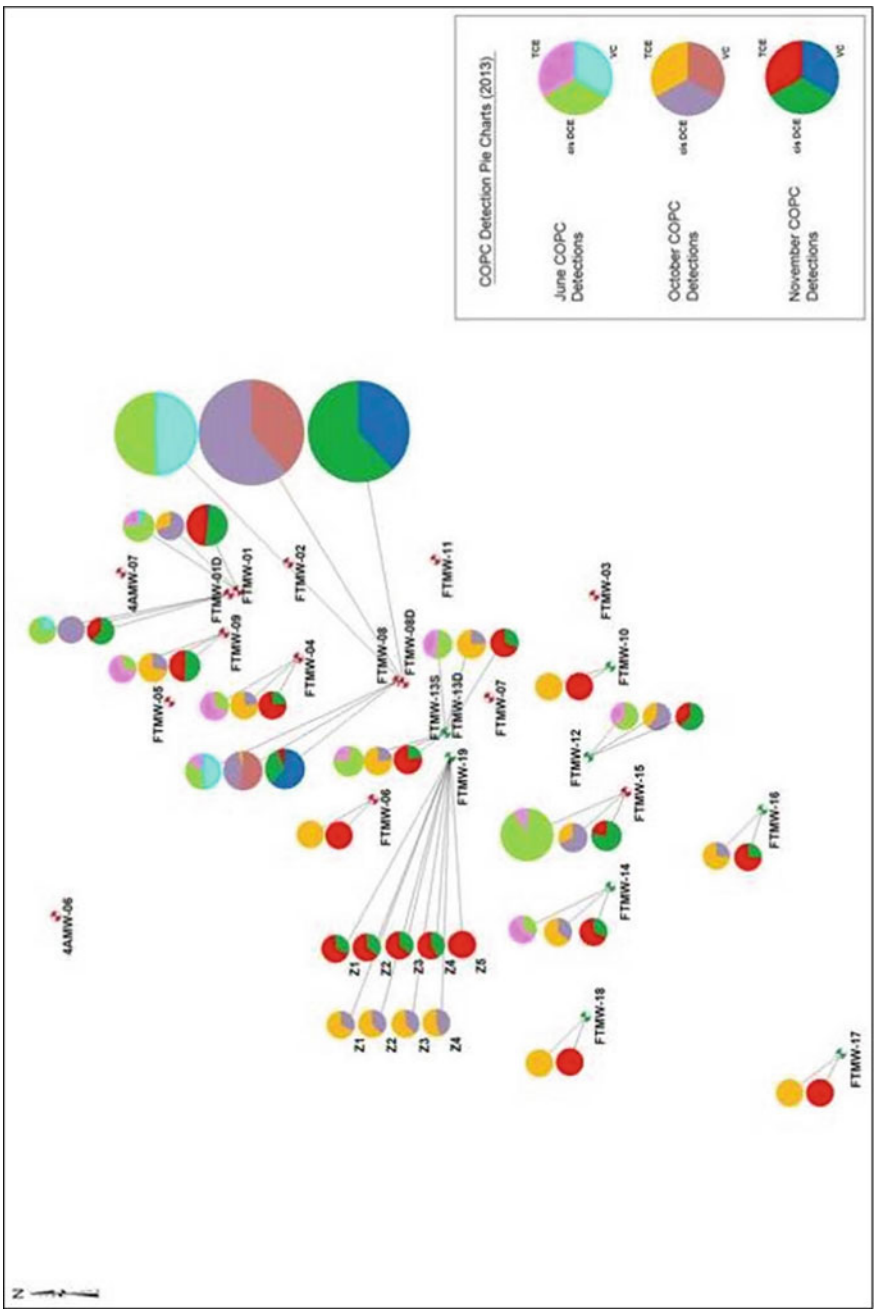

Fig. 7.19 TCE, cis-DCE, and VC pie charts

120 μg/L in November 2013, while the sample in October 2013 had a TCE concentration of 3.8 μg/L. The TCE concentration decrease is also obvious in FTMW-08D and FTMW-06. However, the TCE concentration in FTMW-01 shows fluctuation without a significant decrease. The VC concentration decreases are the most obvious in FTMW-08, FTMW-08D, and FTMW-01, where the VC concentrations in other wells are either in concentrations less than 1 μg/L or non-detects.

Geochemical environmental indicators: Geochemical data can serve as a secondary form of evidence to support natural attenuation. Table 7.10a provides a summary of relevant geochemical data for MNA evaluation. This data encompasses groundwater quality parameters such as redox potential, pH, and dissolved oxygen levels. The data collected at the site indicates that groundwater and soil pH ranges from 6 to 8, indicating a neutral pH level. A pH range between 5 and 9 is generally considered favorable for supporting aerobic degradation of organic compounds. Within the shallow groundwater unit (the overburden aquifer), redox potential varies greatly at the site between − 96 and 189 mV. Also, if ferrous iron is abundant, a redox potential reading could be inaccurate and should not be used to access degradation potential (Interstate Technology and Regulatory Cooperation Work Group [ITRC] 1999). Dissolved oxygen ranged between 0.38 and 8.73 mg/L. Anaerobic bacteria cannot typically survive if the dissolved oxygen is above 0.5 mg/L.

Biological indicators: The presence and activity of the dehalogenating microbes is responsible for each step of the sequential dechlorination of TCE to ethene. Table 7.10b summarizes biological indicator data pertinent to MNA evaluation. While a number of bacterial cultures capable of utilizing PCE or TCE as growth supporting electron acceptors, Dehalococcoides (Dhc) may be the most important ones. They are the only identified bacterial group that is capable of complete reductive dechlorination to ethane. Lu and others (2006) suggest a concentration of 10^4 Dhc cells per milliliter as a screening criterion to identify areas where reductive dechlorination will yield a generally useful biodegradation. Complete reductive dechlorination will be unlikely to occur if Dhc concentrations are less than 10 cells/mL. Like Dhc, the Desulfotomaculum (Dsm) genus is capable of reductively dechlorinating PCE and TCE to cis-DCE (cis-dichloroethylene). What sets Dsm apart from other dechlorinating bacteria is not the range of electron acceptors it can utilize (PCE and TCE), but rather the electron donors that support reductive dechlorination. Dsm species are known to utilize more complex electron donors such as acetate, lactate, pyruvate, and succinate. On the other hand, methanogens utilize hydrogen to produce methane and can therefore compete with dechlorinating bacteria, including Dhc, for available hydrogen resources.

Table 7.10a Field measurement results for MNA parameters

Well ID	Field parameters by multi-parameter instrument						Field analysis by test kits (mg/L)		
	pH	Conductivity	Turbidity	DO	Temperature	ORP	CO_2	Fe^{2+}	H_2S
	(pH units)	(mS/cm)	(NTU)	(mg/L)	(^oC)	(mv)			
4AMW-07	**6.66**	0.676	72	4.46	11.23	152	25	ND	ND
FTMW-03	**6.85**	0.801	10.8	1.18	12.04	129	55	ND	ND
FTMW-06	**6.84**	0.732	0.0	8.61	10.15	166	20	ND	ND
FTMW-08D	**6.95**	0.934	5.9	1.10	10.86	**− 96**	**50**	**3**	ND
FTMW-08	**6.69**	0.820	0.0	7.82	9.21	147	40	ND	ND
FTMW-09	**6.73**	0.698	0.0	4.63	10.75	163	45	ND	ND
FTMW-14	**6.90**	0.781	0.0	7.26	11.96	144	45	ND	ND
4AMW-07	**7.14**	0.601	9.6	5.28	14.04	144	25	ND	ND
FTMW-03	**6.89**	0.688	9.8	3.01	13.95	164	40	ND	ND
FTMW-06	**7.02**	0.636	0.0	3.27	13.77	189	40	ND	ND
FTMW-08D	**7.13**	0.780	9.4	**0.38**	14.98	**− 95**	**60**	**3.4**	ND
FTMW-08	**6.99**	0.753	12.6	0.96	14.16	110	25	ND	ND
FTMW-09	**7.22**	0.601	2.2	8.73	13.82	148	30	ND	ND
FTMW-14	**6.95**	0.639	4.2	2.54	14.46	139	35	ND	ND
Optimal natural attenuation conditions	5–9	2 × background		< 0.5	> 20	< 50	2 × background	> 1	

Values in bold indicate active biodegradation conditions (USEPA 1998)
4AMW-07 is the background well

Table 7.10b Laboratory analysis results for MNA parameters

Well ID	Bacteria analysis results (cells/mL)				Gas analysis results (μg/L)			Geochemical analysis results (mg/L)			
	DHC	DSM	IRB/SRB	MGN	Ethane	Ethene	Methane	Nitrate Nitrite as N	Sulfate	Total iron	TOC
4AMW-07	< 2	< 4	< 3	390	0.0027	**0.033**	0.16	9.2	24	1.5	0.91
FTMW-03	1.0	< 1	231	6930	0.0012	**0.028**	0.039	4.4	32	0.38	1.1
FTMW-06	1.3	< 1	< 0.8	36,000	0.0027	**0.029**	0.026	11	26	0.04	0.67
FTMW-08D	6.7	< 1	**1090**	80,000	**0.01**	**4.6**	**6.4**	**0.099**	120	**5.2**	1.6
FTMW-08	**22.3**	< 1	< 0.8	**465,000**	0.003	**0.077**	0.22	3.2	78	0.044	1.1
FTMW-09	1.8	< 1	< 0.8	5460	0.0035	**0.035**	**0.54**	8.7	26	0.04	0.75
FTMW-14	1.2	< 1	< 0.8	66,900	0.0024	**0.028**	0.05	7.2	42	0.04	0.76
4AMW-07	1.3	< 1	< 0.8	51,200	0.0021	**0.02**	0.17	10	26	0.43	0.84
FTMW-03	2.3	< 1	< 0.8	199,000	**0.032**	**0.026**	0.36	5.7	30	0.052	1
FTMW-06	1.5	< 1	< 0.8	104,000	0.0034	**0.016**	0.2	12	20	0.04	0.77
FTMW-08D	1.0	< 1	< 0.8	41,500	**0.025**	**0.025**	0.1	**ND**	120	**4.3**	1.5
FTMW-08	**42.6**	**2.8**	< 0.8	**1,100,000**	0.0047	**0.088**	**1.3**	1.2	100	0.43	1.4
FTMW-09	6.0	< 1	< 0.8	617,000	0.004	**0.025**	0.14	9.5	26	0.15	0.86
FTMW-14	0.7	< 1	< 0.8	190,000	0.0069	**0.015**	0.36	7.7	38	0.097	0.77
Optimal Natural attenuation conditions	> 10				> 0.01	> 0.01	> 0.5	< 1	< 20	2 × background	> 20

Values in bold indicate active biodegradation conditions (USEPA 1998) conditions
4AMW-07 is the background well
DHC dehalococcoides
DSM desulfuromonas
IRB/SRB iron-reducing bacteria/sulfur reducing bacteria
MGN methanogen

7.5 Pathway-Focused Risk Assessment

A human health risk assessment (HHRA) was performed to establish the initial risks linked to groundwater exposure. The HHRA examined the reasonable maximum exposure (RME) that could potentially occur at the site. The findings of the HHRA are indicative and should serve as a reference when making decisions regarding risk management. In accordance with USEPA (1989) guidance, the HHRA methodology followed the following five elements:

- **Data evaluation and hazard assessment**: The review of available data was conducted to compile datasets for utilization in the risk assessment process. This involved identifying contaminants of potential concern (COPCs) that are closely associated with the site and are detected at a frequency exceeding 5% and concentrations surpassing background levels and/or conservative screening levels. Additionally, exposure point concentrations were calculated to represent the upper-bound conditions of exposure in each affected medium.
- **Exposure assessment**: The human population, i.e., groups potentially exposed to COPCs (referred to as potential human receptors), is characterized. Potential pathways of exposure are identified, specifically those applicable to potential receptors at the site, such as ingestion and inhalation. Estimated COPC exposure concentrations are derived from site-specific monitoring data. The concentrations of COPCs in relevant media, such as groundwater, are converted into systemic doses, considering factors like contact rates (e.g., ingestion rates, exposure frequency, and exposure duration) and absorption rates of each COPC. The magnitude, frequency, and duration of these exposures are then integrated to estimate daily intakes over a specified period, such as a lifetime or activity-specific duration.
- **Toxicity assessment**: The toxicity assessment has two primary objectives: (1) to identify the nature and extent of toxicity associated with each COPC, and (2) to characterize the dose-response relationship, which describes the relationship between the level of exposure and the magnitude of adverse health effects for each COPC. The assessment presents the connection between the extent of exposure and the degree of toxic injury or disease for each COPC. It includes chemical-specific toxicity values, such as cancer slope factors (SFs) and inhalation unit risks (IURs) for carcinogens, as well as reference doses (RfDs) or reference concentrations (RfCs) for non-carcinogens. The scientific basis and derivation of these toxicity values are discussed in detail.
- **Risk characterization**: Risk characterization combines the findings from the toxicity assessment and the exposure assessment to obtain quantitative estimates of human health risk, encompassing both the risk of cancer and non-carcinogenic effects. The US Environmental Protection Agency (USEPA) has established an acceptable target range for cancer risk, which ranges from one in ten thousand

(0.0001 or 10^{-4}) to one in one million (0.000001 or 10^{-6}). Additionally, a non-cancer target hazard level of 1 (USEPA 1991) is defined. During risk characterization, the significant uncertainties and limitations associated with the risk estimates are identified and documented.

- **Uncertainty analysis**: Risk assessment, like any modeling process, involves assumptions and estimates that introduce uncertainty into the results. Uncertainty analysis is an important component of risk assessment as it considers both the variability in measured and estimated parameters and the lack of knowledge surrounding them. By accounting for uncertainty, decision makers can better understand the reliability and limitations of the risk estimates based on the assumptions and data used in the assessment. There are several major sources of uncertainty in risk assessment: (1) Natural variability. This refers to inherent differences among individuals or populations, such as variances in body weight or genetic susceptibility, which can affect the response to a given exposure. (2) Lack of knowledge. Uncertainty arises from gaps in our understanding of basic physical, chemical, and biological properties and processes. For example, limited knowledge about the affinity of a chemical for soil or its solubility in water can introduce uncertainty into exposure estimates. (3) Model accuracy. The models used to estimate key inputs, such as dose-response relationships, may have inherent limitations or uncertainties. These models rely on data from experiments or studies and may not perfectly represent real-world scenarios. (4) Measurement error. Errors in the measurement of exposure levels or biomarkers can introduce uncertainty into the assessment. Among these sources of uncertainty, dose-response relationships and the classification of carcinogenicity based on weight-of-evidence are often associated with greater uncertainties compared to other elements. Extrapolating data from high-dose exposures in animal studies or occupational settings to lower levels of exposure involves numerous assumptions, including effects thresholds, interspecific extrapolation, high- to low-dose extrapolation, and route-to-route extrapolation. The scientific validity of these assumptions is uncertain, and while each individual extrapolation is designed to prevent underestimation of risk, collectively they can result in unquantifiable but potentially significant overestimation of risk. It is important to acknowledge and communicate these uncertainties to ensure that the risk assessment results are appropriately interpreted and used for decision-making purposes.

7.5.1 Exposure Pathway Model

In a Human Health Risk Assessment (HHRA), scenarios are developed to define the conditions under which individuals may be exposed to Contaminants of Potential Concern (COPCs). These scenarios are typically summarized in an Exposure Pathway Model (EPM), which serves as a framework for estimating the risks and hazards associated with each COPC, exposure pathway, and receptor. The preliminary EPM presented in Fig. 7.20 represents understanding of:

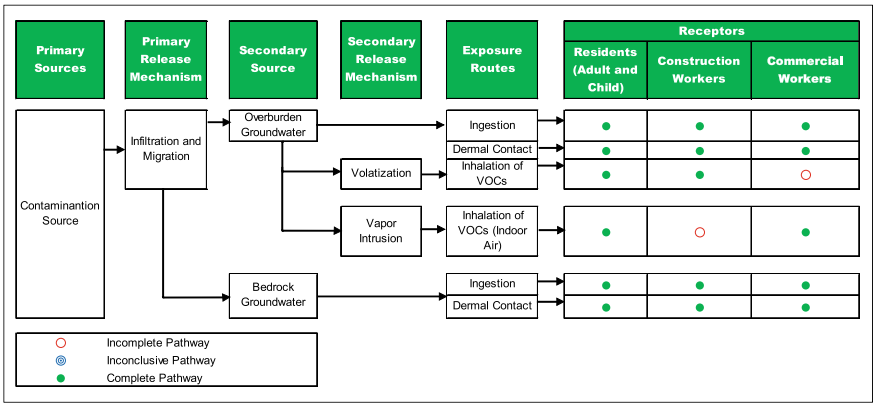

Fig. 7.20 Exposure pathway model for HHRA

- Known or potential sources of COPC in groundwater;
- Primary and secondary release mechanisms that may result in transfer among media;
- Potentially complete exposure pathways for defined receptor populations, based on collected data or expected pathways; and
- Current and potential future on- and off-Site human receptor populations.

7.5.2 Exposure Point Concentrations

Intake serves as a quantitative estimation of the exposure levels. It is determined for each identified complete exposure pathway within the Exposure Pathway Model (EPM) (refer to Fig. 7.20). Intake is expressed as the mass of the substance that comes into contact with the body per unit body weight per unit time. This measurement is typically denoted as milligrams of chemical per kilogram of body weight per day (mg/kg bw-day). The calculation of intakes involves the consideration of several variables. These variables include chemical concentrations, contact rates, exposure frequency, exposure duration, body weight, and exposure averaging time. In the context of the Human Health Risk Assessment (HHRA), exposure point concentrations (EPC) indicate the concentrations of Contaminants of Potential Concern (COPCs) in the relevant environmental media that a selected receptor is expected to come into contact with over a designated exposure period. The reported concentrations of COPCs are used to calculate the 95% upper confidence limit of the mean, following the guidelines provided by the US Environmental Protection Agency (USEPA 1989, 1992). The use of the 95% upper confidence limit (95% UCL) is preferred because assuming long-term contact with the maximum concentration is not considered reasonable according to USEPA guidelines (USEPA 1989). The determination of the 95%UCL is performed using the USEPA ProUCL program (USEPA 2013). The EPC is based on

Table 7.11 Exposure point concentrations of select COPCs

COPC	Mean detected concentration (ug/L)	95% UCL (ug/L)	Maximum detected concentration (ug/L)	EPC value (ug/L)
CIS-DCE	1.91E+02	3.86E+02	2.90E+03	3.86E+02
TCE	3.16E+01	7.72E+01	8.50E+02	7.72E+01
VC	2.09E+02	6.14E+01	8.80E+02	6.14E+01

the lower value between the maximum detected concentration for a specific medium and the 95%UCL. The ProUCL results for cis-DCE, TCE, and VC in groundwater are summarized in Table 7.11.

7.5.3 Exposure Parameters and Exposure Intake Equations

Rates of contact (e.g., ingestion rates, skin surface areas, etc.), exposure frequency and duration, body weight, and averaging time constitute the exposure parameters. The amount of contaminated media contacted per unit time or event is defined as the rate of contact. Exposure frequency and duration are used to determine the duration of exposure to COPCs in the media of concern. The body weight represents the average body weight over an exposure period (USEPA 1989). Tables 7.12, 7.13, 7.14 and 7.15 detail the exposure parameters for the resident adult, resident child, construction worker, and commercial worker, respectively.

7.5.4 Toxicity Assessment for Non-carcinogens

The USEPA provides comprehensive guidance on the methodology used to establish non-cancer reference values or non-carcinogens, as well as considerations for site-specific modifications or applications of these concentrations (USEPA 2014). Non-carcinogens refer to substances that are generally believed to have a threshold daily dose below which harmful effects are unlikely to occur. The concentration associated with this threshold is known as the no-observed-adverse-effect-level (NOAEL). The NOAEL can be derived from various sources, including animal laboratory experiments or human epidemiology investigations, often based on studies conducted in occupational settings. When developing a toxicity value or human NOAEL for non-carcinogens, such as a reference dose (RfD), the regulatory approach involves several steps. First, the critical toxic effect associated with exposure to the chemical is identified, focusing on the most sensitive adverse effect observed. Next, the threshold

Table 7.12 Parameter values for daily groundwater intake of adults

Exposure route	Parameter code	Parameter definition	Units	RME value	Intake equation/ model name
Ingestion	CW	Contaminant concentration in the assessed water	mg/L	EPC table	CDI (mg/kg/day) = CW × CR × EF × ED/(BW × AT) Mutagenic chronic daily intake (MCDI) (mg/kg/day) = CW × EF × [($ED_{6\text{-}16}$ × CR × 3) + ($ED_{16\text{-}30}$ × CR × 1)/BW]/(AT)
	CR	Daily intake rate	L/day	2	
	EF	Annual frequency of exposure	day/ year	350	
	ED-NC	Duration of exposure-noncancer	year	30	
	ED-C	Duration of exposure—cancer	year	24	
	BW	Body weight	kg	70	
	AT-NC	Average time—noncancer	days	10,950	
	AT-C	Average time—cancer	days	25,550	
Dermal	CW	Contaminant concentration in the assessed water	mg/L	EPC table	CDI (mg/kg/day) = DA_{event} × SA × EF × ED × CF/(BW × AT) Mutagenic chronic daily intake (MCDI) (mg/kg/day) = CW × EF × PC × ET × [($ED_{6\text{-}16}$ × SA × 3) + ($ED_{16\text{-}30}$ × SA × 1)/BW] × CF/(AT)
	SA	Surface area for dermal contact	cm^2	18,000	
	PC	Permeability coefficient of the skin	cm/h	Chemical-specific	
	ET	Event time	h/day	0.58	
	EF	Annual frequency of exposure	day/ year	350	
	ED-NC	Duration of exposure— noncancer	year	30	
	ED-C	Duration of exposure—cancer	year	24	
	BW	Body weight	kg	70	
	AT-NC	Average time—noncancer	days	10,950	
	AT-C	Average time—cancer	days	25,550	
	CF	Conversion factor	L/ cm^3	0.001	

(continued)

Table 7.12 (continued)

Exposure route	Parameter code	Parameter definition	Units	RME value	Intake equation/ model name
Inhalation	CA	Contaminant concentration in the air	μg/ m^3	Chemical-specific	Exposure concentration ($\mu g/m^3$) = CA × ET × EF × ED/ AT × CF where, CA = VF × CW Mutagenic chronic daily intake (MCDI) ($\mu g/m^3$) = CA × ET × EF × [($ED_{6\text{-}16}$ × 3) + ($ED_{16\text{-}30}$ × 1)]/ (AT)
	ET	Event time	h/day	24	
	EF	Annual frequency of exposure	day/ year	350	
	VF	Volatilization factor	L/m^3	0.5	
	CF	Conversion factor	h/day	24	
	ED-NC	Duration of exposure—noncancer	year	30	
	ED-C	Duration of exposure—cancer	year	24	
	AT-NC	Averaging time—noncancer	days	10,950	
	AT-C	Average time—cancer	days	25,550	

RME reasonable Maximum Exposure
kg kilogram
CDI chronic daily intake
DA Dermal absorbed dose
mg/L milligrams per liter
h hour
cm^2 square centimeter
$\mu g/m^3$ micrograms per cubic meters
L/m^3 liters per cubic meter

dose is identified from either animal or human studies. Finally, this dose is modified to account for factors such as interspecies variability (when applicable), differences in individual sensitivity (within-species variability), and other uncertainties and modifying factors.

For the derivation of the Reference Concentration (RfC), experimental exposures are extrapolated to a Human Equivalent Concentration (HEC). This process involves two steps: the determination of a point of departure (POD) and the adjustment of the POD by a Dosimetric Adjustment Factor (DAF). The POD can be based on various measurements, such as a No-Observed-Adverse-Effect-Level (NOAEL), Lowest-Observed-Adverse-Effect-Level (LOAEL), benchmark concentration, lower confidence limit, or the lower limit on an effective concentration using a 10% response level (LEC10). The DAF is specific to the site in the body where the toxic effects of the chemical occur, such as the respiratory tract.

Uncertainty factors (UFs) are employed to address the inherent uncertainties involved in extrapolating data. Typically, UFs are default factors of tenfold used in deriving the Reference Concentration (RfC) and Reference Dose (RfD) from experimental data. However, UFs lower than 10 can also be utilized depending on the

Table 7.13 Parameter values for daily groundwater intake of children

Exposure route	Parameter code	Parameter definition	Units	RME value	Intake equation/ model name
Ingestion	CW	Contaminant concentration in the assessed water	mg/L	EPC table	CDI (mg/kg/day) = $CW \times CR \times EF \times ED/(BW \times AT)$ Mutagenic chronic daily intake (MCDI) (mg/kg/day) = $CW \times EF \times ([(ED_{0\text{-}2} \times CR \times 10) + (ED_{2\text{-}6} \times CR \times 3)]/BW)/(AT)$
	CR	Daily intake rate	L/day	1	
	EF	Annual frequency of exposure	day/ year	350	
	ED	Duration of exposure	year	6	
	BW	Body weight	kg	15	
	AT-NC	Average time—noncancer	days	2190	
	AT-C	Average time—cancer	days	25,550	
Dermal	CW	Contaminant concentration in the assessed water	mg/L	EPC table	CDI (mg/kg/day) = $DA_{event} \times SA \times EF \times ED/(BW \times AT)$ Mutagenic chronic daily intake (MCDI) (mg/kg/day) = $CW \times EF \times PC \times ET \times CF \times ([(ED_{0\text{-}2} \times SA \times 10) + (ED_{2\text{-}6} \times SA \times 3)]/BW)/(AT)$
	SA	Surface area for dermal contact	cm^2	6600	
	PC	Permeability coefficient of the skin	cm/h	Chemical-specific	
	ET	Event time	h/day	1	
	EF	Exposure frequency	day/ year	350	
	ED	Duration of exposure	year	6	
	BW	Body weight	kg	15	
	AT-NC	Average time—noncancer	days	2190	
	AT-C	Average time—cancer	days	25,550	
	CF	conversion factor	L/cm^3	0.001	

circumstances. In certain cases, a UF of 3 can be employed instead of the standard one-half power ($10^{0.5}$) when deemed appropriate. UFs are utilized to account for the following sources of uncertainty: (1) Variability in susceptibility among individuals in the human population, known as inter-individual or intra-species variability, (2) Uncertainty when extrapolating animal data to humans, referred to as interspecies uncertainty, (3) Uncertainty when extrapolating from subchronic to chronic exposure scenarios, (4) Uncertainty when extrapolating from a Lowest Observed Adverse Effect Level (LOAEL) rather than a No-Observed-Adverse-Effect Level (NOAEL),

Table 7.14 Parameter values for daily groundwater intake of construction workers

Exposure route	Parameter code	Parameter definition	Units	RME value	Intake equation/ model name
Ingestion	CW	Contaminant concentration in the assessed water	mg/L	EPC table	CDI (mg/kg/day) = CW × CR × EF × ED/(BW × AT)
	CR	Daily intake rate	L/day	0.05	
	EF	Annual frequency of exposure	day/ year	50	
	ED	Duration of exposure	year	1	
	BW	Body weight	kg	70	
	AT-NC	Average time—noncancer	days	365	
	AT-C	Average time—cancer	days	25,550	
Dermal	CW	Contaminant concentration in the assessed water	mg/L	EPC table	CDI (mg/kg/day) = DA_{event} × SA × EF × ED × CF/ (BW × AT)
	SA	Surface area for dermal contact	cm^2	3300	
	PC	Permeability coefficient of the skin	cm/h	Chemical-specific	
	ET	Event time	h/day	4	
	EF	Annual frequency of exposure	day/ year	50	
	ED	Duration of exposure	year	1	
	BW	Body weight	kg	70	
	AT-NC	Averaging time—noncancer	days	365	
	AT-C	Averaging time—cancer	days	25,550	
	CF	Conversion factor	L/ cm^3	0.001	
Inhalation	CA	Contaminant concentration in the air	mg/ m^3	Chemical-specific	Exposure concentration (μg/ m^3) = CA × ET × EF × ED/AT × CF
	ET	Event time	h/day	4	
	EF	Annual frequency of exposure	day/ year	50	
	CF	Conversion factor	h/day	24	

(continued)

Table 7.14 (continued)

Exposure route	Parameter code	Parameter definition	Units	RME value	Intake equation/ model name
	ED	Duration of exposure	year	1	
	AT-NC	Averaging time—noncancer	days	365	
	AT-C	Averaging time—cancer	days	25,550	

(1) Construction workers ingestion of groundwater is incidental and assumed at 5% of the industrial worker ingestion rate
(2) It is assumed that construction workers come into contact with groundwater only once a week
(3) Construction events are assumed to have a maximum duration of one year
(4) Contact with groundwater is limited to specific body parts, namely the head, hands, and forearms, as construction workers are expected to wear short-sleeved shirts, long pants, and shoes
(5) During construction events, it is assumed that contact with groundwater occurs for half of the time spent on the construction site each day

and (5) Uncertainty associated with incomplete data. The maximum UF for deriving RfCs in this context is 3000, while the maximum UF for deriving RfDs is 1000. Modifying factors (MFs) are also considered, taking into account the confidence in the scientific studies used to derive toxicity values. The combination of UFs and MFs ensures a conservative and protective approach in the derivation of RfCs and RfDs from available data for human health risk assessments (HHRA).

MF is incorporated in the risk assessment process to account for additional uncertainties in the critical study and the overall database that are not addressed by the uncertainty factors. It is a qualitative professional assessment that ranges from 1 to 10. The default value for the MF is 1, indicating no additional adjustment. However, it is important to note that the USEPA discontinued the use of the modifying factor in 2004. However, toxicity values derived before 2004 may still contain a modifying factor if they were developed using the previous methodology. In addition, the oral RfD for manganese contains an MF of 3 based upon guidance set forth by USEPA (USEPA 2014).

The RfD is determined by dividing the relevant NOAEL by the product of all applicable UFs and the MF. This is expressed in units of mg/kg-day and is calculated as Eq. 7.5:

$$\text{RfD} = \text{NOAEL}/(\text{UF}_1 \times \text{UF}_2 \cdots \times \text{MF}) \tag{7.5}$$

The resulting RfD is expressed in units of milligrams of chemical per kilogram of body weight per day (mg/kg-bw/day).

For the inhalation pathway, an RfC is calculated. To calculate the RfC, the human equivalent concentration (HEC) is divided by UFs and is expressed in units of mg/m^3 (Eq. 7.6).

Table 7.15 Parameter values used for daily groundwater intake of commercial workers

Exposure route	Parameter code	Parameter definition	Units	RME value	Intake equation/ model name
Ingestion	CW	Contaminant concentration in the assessed water	mg/L	EPC table	CDI (mg/kg/day) = CW × CR × EF × ED/(BW × AT)
	CR	Daily intake rate	L/day	1	
	EF	Annual frequency of exposure	day/ year	250	
	ED	Duration of exposure	yr	25	
	BW	Body weight	kg	70	
	AT-NC	Average time—noncancer	days	9125	
	AT-C	Average time—cancer	days	25,550	
Dermal	CW	Contaminant concentration in the assessed water	mg/L	Chemical-specific	CDI (mg/kg/day) = DA_{event} × SA × EF × ED × CF/(BW × AT)
	SA	Surface area for dermal contact	cm^2	1980	
	PC	Permeability coefficient of the skin	cm/h	Chemical-specific	
	ET	Event time	h/day	0.5	
	EF	Annual frequency of exposure	day/ year	250	
	ED	Duration of exposure	year	25	
	BW	Body weight	kg	70	
	AT-NC	Average time—noncancer	days	9125	
	AT-C	Average time—cancer	days	25,550	
	CF	conversion factor	L/cm^3	0.001	

(1) Assumes the commercial worker dermal contact is limited to hand and lower forearm
(2) Total washing time based on an 8-h workday

$$\mathrm{RfC} = \mathrm{HEC}/(\mathrm{UF}_1 \times \mathrm{UF}_2 \cdots) \tag{7.6}$$

7.5.5 *Toxicity Assessment for Carcinogenicity*

Carcinogens are different from non-carcinogens in that they are generally believed to have no threshold. It is presumed that there is no level of exposure below which carcinogenic effects will not occur. This concept of a "non-threshold" is based on the understanding that even small levels of exposure to a potential carcinogen carry a finite probability of inducing a carcinogenic response.

The USEPA utilizes a two-part evaluation approach to assess carcinogenic effects. This approach involves assigning a weight-of-evidence classification and quantifying the cancer toxic potency concentration (EA Engineering, Science, and Technology, Inc. 2021). The quantification is expressed through a slope factor (SF) for oral and dermal exposures and an inhalation unit risk (IUR) for inhalation exposures. These factors reflect the dose-response relationship observed in the available data for the specific carcinogenic endpoint(s) (USEPA 1989).

To communicate the hazard associated with carcinogens, the USEPA has established five recommended standard hazard descriptors: "Carcinogenic to Humans," "Likely to Be Carcinogenic to Humans," "Suggestive Evidence of Carcinogenic Potential," "Inadequate Information to Assess Carcinogenic Potential," and "Not Likely to Be Carcinogenic to Humans" (USEPA 2005). The weight-of-evidence classification is determined through a comprehensive scientific evaluation of the available data. Only compounds that receive a weight-of-evidence classification of C or above are considered to have carcinogenic potential in the risk assessment process.

The weight-of-evidence classifications established by the USEPA (USEPA 1989) and currently displayed in the toxicity profiles on the IRIS system were utilized for interpreting the carcinogenic toxicity of Concerned Organic Pollutants and Contaminants (COPCs) due to the incomplete integration of the revised cancer guidelines (USEPA 2005) into the IRIS chemical profiles. The weight-of-evidence classification system assigns a letter or alphanumeric code (A through E) to each potential carcinogen, indicating its assessed potential to cause cancer in humans.

Assessing the potential carcinogenic effects involves the utilization of slope factors (SF) for oral and dermal exposures, as well as inhalation unit risks (IUR) for inhalation exposures. These factors are derived from observed dose-response relationships for specific carcinogenic endpoints (USEPA 1989). SF and IUR represent the upper 95th percentile confidence limit of the probability of an individual experiencing a response per unit daily intake of a chemical throughout their lifetime. The SF is measured as the proportion of the population affected per milligram/kilogram per day, while the IUR is expressed in micrograms per cubic meter ($\mu g/m^3$). Their primary purpose is to estimate the upper-bound lifetime probability of an individual developing cancer due to exposure to a specific concentration of a carcinogen. Typically, SFs and IURs are derived from experimental animal data, unless suitable epidemiological studies are available. However, detecting and measuring carcinogenic effects at low exposure concentrations pose challenges. Therefore, SFs and IURs are developed by fitting a model to the available high-dose experimental animal data and extrapolating it to the low-dose range, which is more representative of human

exposure. The linear multistage model is recommended by the USEPA as a conservative approach that provides an upper bound estimate of excess lifetime cancer risk. For more comprehensive information on these methods and approaches, please refer to the USEPA Cancer Guidelines (USEPA 2005).

Apart from evaluating the carcinogenic effects of compounds, it is also important to assess their mutagenic modes of action. Some specific compounds of potential concern (COPCs), such as TCE and VC, have been identified as having mutagenic properties. When considering exposures during early life and the mutagenic mode of action, adjustments are made to cancer potency estimates. In situations where there is a lack of chemical-specific data, the USEPA recommends a default approach that utilizes estimates from chronic studies, known as cancer slope factors, with appropriate modifications to account for the potential differential risk associated with early-life exposure (USEPA 2005). This adjustment is necessary because studies have indicated that a given exposure occurring early in life poses a higher cancer risk compared to the same exposure during adulthood (USEPA 2005). Therefore, for this human health risk assessment (HHRA), the intakes of methylene chloride, TCE, and VC are adjusted in accordance with the guidelines provided by the USEPA (2005).

In this HHRA, only the resident population falls within the age range that necessitates adjustment for a mutagenic mode of action. The residential scenario considers two age groups: adults and children. The child age group is assumed to be from 0 to 6 years old, while the adult age group spans from 7 to 30 years old (USEPA 1991). Although adults are typically considered to be older than 16 years of age, the resident adult in this assessment is evaluated for long-term exposure, which is characteristic of residents (USEPA 1991). Since residents are assumed to have a duration of exposure of 30 years, the resident adult age range extends from 7 to 30 years beyond childhood (USEPA 1991). Therefore, both the resident child and the resident adult require adjustment for potential mutagenic modes of action in this HHRA.

7.5.6 Toxicity Assessment for TCE

The USEPA released a Toxicity Assessment for TCE in 2011. Carcinogenic SFs and IURs are presented for based on three separate target tissue sites—kidney, lymphoid tissue, and liver. Within IRIS, one SF and IUR is presented for TCE that represents the sum of the SF and IUR estimates for the three individual cancer types (USEPA 2014). Additionally, TCE is identified with a mutagenic mode of action for the kidney only. Therefore, application of the mutagenic adjusted DAF to the summed SF and IUR presented in IRIS results in an over-estimate of cancer risk estimates for TCE. According to the Integrated Risk Information System (IRIS) guidelines, the risk assessment for kidney cancer should be conducted using the mutagenic equations. On the other hand, the risk assessments for liver cancer and non-Hodgkin lymphoma (NHL) should be addressed using the standard cancer intake equations (USEPA 2014). To determine cancer risk estimates for the resident adult and child exposure to TCE, the following steps were performed:

- Calculate the TCE intake with the mutagenic mode of action to incorporate the adjusted DAF based on kidney mutagenic endpoint [IUR of 1×10^{-6} $(\mu g/m^3)^{-1}$ and oral SF of 9.3×10^{-3} $(mg/kg/day)^{-1}$].
- Calculate a TCE intake based on non-kidney (NHL/liver) cancer endpoint [IUR of 3.1×10^{-6} $(\mu g/m^3)^{-1}$ and oral SF of 3.7×10^{-2} $(mg/kg/day)^{-1}$]. These toxicity values represent the sum of the NHL and liver IUR and SF.

Therefore, two separate intakes for carcinogenic effects are presented for TCE. One intake is based upon the kidney endpoint and takes into account an adjusted DAF for a mutagenic mode of action. The second intake is based upon the NHL/liver endpoint and does not have an adjustment for a mutagenic mode of action. Intakes for non-carcinogenic effects are based upon a single endpoint and are not modified as discussed above.

7.5.7 Risk Characterization

In the risk characterization process, the aim is to assess the potential risks associated with human exposure to contaminants of potential concern (COPCs) in groundwater. This involves summarizing and integrating the chemical intake levels and toxicity values to provide quantitative expressions of risk. By doing so, a numerical representation of the risk level for human contact with COPCs in groundwater can be obtained. To evaluate potential non-carcinogenic effects, the chemical intake levels are compared to the corresponding toxicity values. This comparison allows for an assessment of the potential for non-carcinogenic health effects resulting from exposure to COPCs. For potential carcinogenic effects, the risk characterization involves estimating the incremental probabilities of an individual developing cancer over a lifetime of exposure. This estimation is based on the chemical intake levels and specific dose-response information for each chemical. The dose-response information includes parameters such as slope factors (SFs) and inhalation unit risks (IURs), which reflect the relationship between the dose of a carcinogen and the likelihood of developing cancer. Separate discussions are conducted for carcinogenic and non-carcinogenic effects due to the differing methodologies used to assess these two modes of chemical toxicity.

Hazard index for non-carcinogenic effects: To assess the potential human health risks associated with exposures to non-carcinogenic COPCs, a comparison is made between the average daily intake (ADI) and the chemical-specific RfD or RfC. A hazard quotient (HQ) is derived for each COPC, as shown in Eq. 7.7:

$$\mathrm{HQ} = \frac{\mathrm{ADI}}{\mathrm{RfD}} \quad \text{or} \quad \mathrm{HQ} = \frac{EC}{\mathrm{RfC} \times 1000\ \mu g/m^3} \tag{7.7}$$

where, HQ indicates the Hazard Quotient, which is a dimensionless ratio defined as the average daily intake level divided by the acceptable daily intake level. ADI

represents the calculated non-carcinogenic average daily intake in mg/kg/day. The RfD denotes the reference level for oral and dermal exposure, which is also expressed in mg/kg/day. The *EC* is the concentration of a contaminant ($\mu g/m^3$), and RfC is the reference level for inhalation exposure, expressed in mg/m^3.

When the ADI of a chemical exceeds the RfD or RfC, the HQ value will be greater than 1.0. This suggests a potential concern for adverse systemic health effects in the populations exposed to the chemical. Conversely, if the ADI is below the RfD or RfC, the HQ value will be below 1.0, indicating no immediate concern for adverse systemic health effects in the exposed populations. However, if the sum of multiple HQ values exceeds 1.0, and these compounds affect the same target organ, there may be a concern for potential adverse systemic health effects in the exposed populations. This implies that the combined exposure to multiple chemicals may have a cumulative effect on the target organ, increasing the likelihood of adverse health effects. It is important to note that the HQ value represents the level of concern but does not provide a statistical probability of adverse health effects occurring.

When multiple chemicals are present and can cause systemic toxicity through different pathways, the individual Hazard Quotients (HQs) can be combined to calculate an overall Hazard Index (HI). The HI provides an assessment of the potential health effects associated with exposures at the site. If the calculated HI is below 1.0, it suggests that the exposures are unlikely to cause adverse health effects. However, if the total HI exceeds 1.0, it indicates that further analysis is required. In such cases, separate HIs can be calculated for specific toxic endpoints or target organs of concern. For instance, the HQs for neurotoxic compounds can be summed separately from the HQs for renal toxins. By calculating endpoint-specific HIs, a more detailed evaluation can be conducted to determine if there is a reason for concern regarding potential health effects associated with a specific endpoint. This approach allows for a focused assessment of the potential risks related to specific health endpoints, providing a more comprehensive understanding of the overall health risk.

Carcinogenic risks: Carcinogenic risk is determined as the increased probability of an individual developing cancer throughout their lifetime due to exposure to a potential carcinogen. The numerical estimation of the additional lifetime cancer risk is obtained by multiplying the Lifetime Average Daily Intake (LADI) by the risk per unit dose, which is represented by either the Slope Factor (SF) or the Inhalation Unit Risk (IUR). This is shown in Eq. 7.8:

$$\begin{cases} \text{Risk} = \text{LADI} \times \text{SF} \\ \text{Risk} = EC \times \text{IUR} \end{cases} \tag{7.8}$$

where, Risk is the unitless probability of an exposed individual developing cancer; LADI is the lifetime cancer average daily intake (mg/kg-day or ug/m^3); SF is the cancer slope factor $(mg/kg\text{-}day)^{-1}$; *EC* is the exposure concentration ($\mu g/m^3$); and IUR is the inhalation unit risk $(\mu g/m^3)^{-1}$.

Because the SF and the IUR are the statistical 95th percent upper-bound confidence limit on the dose-response slope, this method provides a conservative, upper-bound estimate of risk. The carcinogenic risk thresholds are defined as cumulative carcinogenic risks that exceed the risk range of 1 in 1 million (1×10^{-6}) to 1 in 10,000 (1×10^{-4}).

According to Table 7.16, the HHRA evaluated the potential cumulative risks associated with groundwater exposure for different populations, including residents (adult and child), construction workers, and commercial workers. The assessment considered ingestion, dermal contact, and inhalation of VOCs present in groundwater. For the resident (adult and child) and commercial worker, the non-carcinogenic hazards exceeded a HQ of 1.0, indicating potential risks. Specifically, cis-DCE, TCE, and VC had chemical-specific HQs greater than 1.0. Additionally, the liver, kidney, and immunological system had Hazard Indices (HIs) greater than 1.0, suggesting potential adverse effects on these systems. The incremental lifetime carcinogenic risks for the resident (adult and child combined) and the commercial worker were found to be above the upper end of the risk threshold range (10^{-6}–10^{-4}) set by the USEPA. TCE and VC were identified as having carcinogenic risks above 10^{-4}, indicating significant concerns regarding their potential to cause cancer. Concerns were raised about the use of groundwater as a tap water source due to these findings. Furthermore, the resident adult was evaluated for potential concerns related to VOC vapor intrusion from groundwater into indoor air. The USEPA Johnson and Ettinger model suggested that volatilization of Contaminants of Potential Concern (COPCs) in groundwater into site buildings could be a potential concern (USEPA 2004). Specifically, TCE had a non-cancer HQ greater than 1.0, indicating a potential risk.

The construction worker's exposure to groundwater, including incidental ingestion, dermal contact, and inhalation while in a trench, was found to be below the risk thresholds established by the USEPA. Therefore, the risks associated with groundwater exposure for the construction worker were deemed to be acceptable.

7.5.8 Risk Assessment Uncertainty

Analyzing uncertainties is crucial in exposure assessment, providing risk assessors and reviewers with information on individual uncertainties linked to exposure factor assumptions and their potential impact on the final assessment. Conservative assumptions are employed regarding exposure to groundwater, potentially leading to an overestimation of potential health risks. For this HHRA, the most conservative land use scenario (residential) is included in the evaluation. Groundwater within the site is assumed as a tap water source although public water is available. In addition, the HHRA does not take into account any restrictions on groundwater use or exposure. Exposure parameters (e.g., body weight, ingestion rates, time spent in one place, etc.) used in estimating COPC intakes are a combination of an average and upper bound levels taken from USEPA sources. The use of upper-bound estimates tends to overestimate exposure; therefore, the potential risks presented in the HHRA are

Table 7.16 Summary of HHRA carcinogenic risks and noncarcinogenic hazards

Receptor	Exposure pathway	Carcinogenic risks	Non-carcinogenic hazards	COPC contributing significantly to results
Child resident	Ingestion	1.3×10^{-3}	25	VC, TCE, cis-DCE
	Dermal contact	1.8×10^{-4}	5.4	VC, TCE, cis-DCE
	Inhalation	–	–	Not applicable
	Cumulative results	**1.5×10^{-3}**	**30**	VC, TCE, cis-DCE
Adult resident	Ingestion	8.0×10^{-4}	11	VC, TCE, cis-DCE
	Dermal contact	1.2×10^{-4}	2.3	VC, TCE, cis-DCE
	Inhalation	2.3×10^{-4}	23	TCE
	Cumulative results	**1.2×10^{-3}**	**36**	
Adult and child resident (combined)	Ingestion	2.1×10^{-3}	–	VC, TCE, cis-DCE
	Dermal contact	3.0×10^{-4}	–	VC, TCE, cis-DCE
	Inhalation	2.3×10^{-4}	–	VC, TCE, cis-DCE
	Total risk across groundwater (adult and child)	**2.6×10^{-3}**	**–**	VC, TCE, cis-DCE
	Total risk across all media and all exposure routes (adult and child)	**3×10^{-3}**	**–**	VC, TCE, cis-DCE
	Total hazard index across all media and all exposure routes (child)	**–**	**30**	VC, TCE, cis-DCE
	Total hazard index across all media and all exposure routes (adult)	**–**	**36**	VC, TCE, cis-DCE
Construction worker	Ingestion	7×10^{-8}	0.04	Not applicable
	Dermal contact	3×10^{-7}	0.2	Not applicable
	Inhalation	1×10^{-13}	0.000006	Not applicable
	Cumulative results	**1×10^{-6}**	**0.2**	
Commercial worker	Ingestion	2×10^{-4}	3.8	VC, TCE, cis-DCE

(continued)

Table 7.16 (continued)

Receptor	Exposure pathway	Carcinogenic risks	Non-carcinogenic hazards	COPC contributing significantly to results
	Dermal contact	6×10^{-6}	0.2	VC
	Inhalation	–	–	Not applicable
	Cumulative results	$\mathbf{2 \times 10^{-4}}$	**4**	

likely to be greater than actual risks. However, the residential exposure to groundwater presents a baseline exposure assessment that should be taken into account for any risk management decisions made for the site.

7.6 Cost-Effective Approach for Groundwater Contamination Induced Risk Mitigation

Aquifer remediation is necessary when the risks associated with groundwater contamination exceed acceptable levels. The primary objectives of aquifer remediation can be summarized as follows:

Health protection: The remediation aims to prevent exposure to groundwater contamination at concentrations that pose risks above acceptable levels. This objective focuses on safeguarding human health by ensuring that the groundwater is free from contaminants or that exposure pathways are effectively eliminated.

Plume containment: Another objective is to prevent or minimize the further migration of the contaminant plume. This involves implementing measures to contain the spread of contamination within the aquifer and prevent its migration to unaffected areas. By containing the plume, the remediation efforts limit the potential for additional contamination and reduce the overall extent of the affected area.

Source control: The remediation seeks to prevent or minimize the migration of contaminants from source materials (such as contaminated soil or waste sites) into the groundwater. Source control measures focus on addressing and mitigating the primary sources of contamination to prevent ongoing or future contamination of the aquifer.

Aquifer restoration: Wherever practicable, the objective of aquifer remediation is to restore the groundwater to its expected beneficial uses. This involves reducing contaminant concentrations to acceptable levels and ensuring that the aquifer can support its intended uses, such as drinking water supply, irrigation, or industrial purposes.

Figure 7.21 presents a decision framework for selecting remediation methods in karst aquifers. The framework emphasizes the importance of addressing source materials, which typically contain the highest concentrations of contaminants. Remediation measures focused on removing or addressing these source materials are considered to provide the greatest value in terms of contaminant reduction per unit of expenditure. Source control measures, such as removal or containment of the source materials, are often considered cost-effective steps in groundwater restoration programs. Pathway elimination is another valuable approach in karst aquifers. While it doesn't directly address the contaminated groundwater, eliminating the exposure pathway by using an alternative water supply source can prevent receptors from being exposed to the contaminated groundwater. Treating impacted groundwater is a well-researched topic, and various technologies are available for addressing contamination in karst aquifers. However, the selection of the most appropriate method should consider the site-specific conditions, as each karst aquifer has unique hydrogeological characteristics and contaminant distribution. Technical impracticability is regarded as a last resort in the decision framework. It suggests that a regulatory waiver for remediation requirements may only be granted when other options have been thoroughly evaluated and proven to be impractical or unfeasible. Based on the information provided, managing impacted groundwater appears to be the most applicable remediation option for the study site within the context of the decision framework presented in Fig. 7.21.

In Fig. 7.22, specific techniques are depicted for each remediation option, along with an outline of the associated challenges. The management of impacted groundwater encompasses various technologies, including pump and treat, permeable reactive barriers, enhanced chemical oxidation and/or bioremediation, as well as monitoring of natural attenuation. Historically, pump and treat has been widely employed for groundwater remediation and management. However, there has been a recent shift towards the adoption of in-situ technologies. Considering the hydrogeological conditions and the delineated extents of COPCs in both the overburden and bedrock formations, alternative approaches for groundwater remediation included in-situ chemical oxidation and enhanced bioremediation. It is important to note that monitored natural attenuation plays a significant role in these remediation techniques.

7.7 Summary

Groundwater contamination was identified in the unconsolidated overburden and the underlying karst formations at the study site. The overburden aquifer is comprised of silt and clay, with varying thicknesses ranging from 13 to 129 feet. On the contrary, the karst aquifer consists of carbonate rock, characterized by an irregular surface, water-filled or clay-filled voids, and discrete fracture zones. Within the bedrock aquifer, significant variations in specific capacity and hydraulic conductivity have been observed, along with the coexistence of confined and unconfined conditions. The presence of preferential flow pathways and interconnected fractures further adds

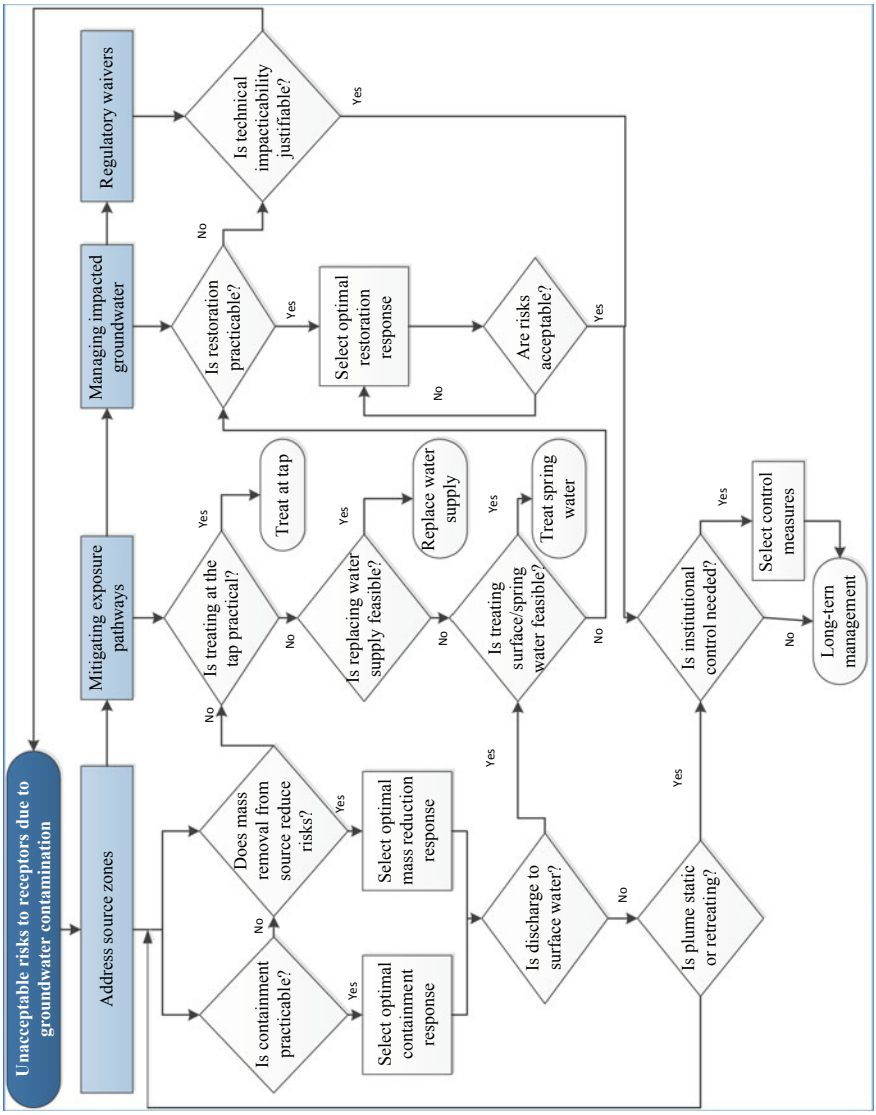

Fig. 7.21 Decision framework of addressing contaminated groundwater in karst aquifers (Randrianarivelo et al. 2019)

Karst Aquifer Remediation Strategy	Remediation Techniques	Challenges
Address source zones: reduce mass flux into the aquifer to the extent practicable	❑ Soil excavation (most common) ❑ Mass reduction via NAPL removal (Commonly employed with pooled NAPL) ❑ Mass reduction via vapor removal ❑ Physical, chemical, or hydraulic containment ❑ In-situ remediation technologies	❑ Much of the mass may reside in the epikarst or underlying bedrock and be inaccessible to excavation ❑ Volumes of pooled NAPL may be large due to the high porosity of the epikarst. Accumulation may be more episodic than continual ❑ Air-filled, interconnected nature of many epikarsts lend themselves to epikarst vapor extraction technology ❑ Pumping wells cannot be relied upon to effect capture; capture zones cannot be reliably modeled using numerical codes such as MODFLOW ❑ Often costly and challenging to construct any hydrogeologic barriers in karst
Mitigating exposure pathways: perhaps the most useful active remedial component in karst	❑ Treating at the tap ❑ Replacing potable water supplies ❑ Treating spring water by capturing and treating spring flow or "passive"" treatment by constructing a treatment wetland or filtration system ❑ Land use control including fences, signage, deed restrictions, local ordinances	❑ Long-term operation and maintenance costs ❑ Costs can be offset somewhat if treatment of groundwater between the source and the potential receptors is not attempted ❑ Water from more than one spring needs to be treated ❑ Spring biota will likely be affected and requires an evaluation ❑ Educate people of land use control as a component of remedies
Managing impacted groundwater	❑ Pump and treat ❑ Permeable reactive barriers ❑ Spot treatment using enhanced chemical oxidation, enhanced bioremediation, thermal destruction ❑ Monitored Natural Attenuation ❑ Performance Monitoring	❑ Primary challenge is to identify the zone requiring treatment ❑ Effective technologies tailored to site conditions and specific contaminants ❑ An appropriate monitoring approach and high-quality monitoring data are critical to evaluate effectiveness. ❑ Monitoring locations consist of springs, streams, extraction systems (if any), and monitoring wells previously shown by testing to be relevant ❑ Water-quality sampling may need to be based on precipitation events
Regulatory waivers	❑ Not applicable	❑ Justification requirements: complex hydrogeology, dense non-aqueous phase liquids, or diffusion- limited or sorption limited contaminant behavior ❑ Given the uncertainty of karst, a robust, karst-specific monitoring program would still be required

Fig. 7.22 Remediation strategies for karst aquifers and their challenges (Randrianarivelo et al. 2019)

to the complexity. The presence of karst features has made it challenging to determine both the vertical and lateral extents of contamination plumes. However, a phased approach involving multiple disciplines and techniques made it possible to successfully delineate the groundwater contamination in both formations. To assess potential risks associated with exposure to contaminated groundwater, a human health risk assessment (HHRA) was conducted. The assessment evaluated the cumulative risks for residents (including adults and children), construction workers, and commercial workers. The results of the HHRA indicate concerns regarding the use of groundwater as a source of tap water. There is also a potential concern for the volatilization of Contaminants of Potential Concern (COPCs) from groundwater into site buildings. However, the results for construction worker exposure to groundwater are below the established risk thresholds. Despite the lower risks for construction workers, the unacceptable health risks identified for residents and other individuals have necessitated the remediation of groundwater. Two viable alternatives for groundwater remediation including in-situ chemical oxidation and in-situ enhanced bioremediation have been identified to mitigate the unacceptable risks. It is worth noting that monitored natural attenuation is considered a common component of the selected remedy, playing a crucial role in the overall remediation process.

References

Arnold WA, Roberts AL (2000) Pathways and kinetics of chlorinated ethylene and chlorinated acetylene reaction with Fe(0) particles. Environ Sci Technol 34:1794–1805

Butler EC, Hayes KF (1999) Kinetics of the transformation of trichloroethylene and tetrachloroethylene by iron sulfide. Environ Sci Technol 33:2021–2027

EA Engineering, Science, and Technology, Inc. (2021) Human health risk assessment: remedial investigation American Creosote Deridder Superfund Site Deridder, Beauregard Parish, Louisiana EPA Identification No. LAN000604293. https://semspub.epa.gov/work/06/100023204.pdf?cv=1. Accessed 20 Sept 2023

Environmental Security Technology Certification Program (2011) Guidance protocol: environmental restoration project ER-0518, application of nucleic acid-based tools for monitoring monitored natural attenuation (MNA), biostimulation, and bioaugmentation at chlorinated solvent sites

Ferrey M, Wilson JT (2002) Complete natural attenuation of PCE and TCE without the accumulation of vinyl chloride. In: Third international conference on remediation of chlorinated and recalcitrant compounds, Monterey, CA

Gelhar LW, Welty C, Rehfeldt KR (1992) A critical review of data on field-scale dispersion in aquifers. Water Resour Res 28(7):1955–1974

Groundwater Sciences Corporation (2011) Supplemental remedial investigation groundwater report (Part 1). https://www.yorksiteremedy.com/Documents/Final%20Supl%20RI%20GW%20Rprt-Sept2011.pdf?cv=1. Accessed 20 Nov 2023

He YT, Wilson JT, Su C, Wilkin RT (2015) Review of abiotic degradation of chlorinated solvents by reactive iron minerals in aquifers. Groundwater Monitor Remed 35(3):57–75. https://doi.org/10.1111/gwmr.12111

Interstate Technology and Regulatory Cooperation Work Group (1999) natural attenuation of chlorinated solvents in groundwater: principles and practices

Jeong H, Hayes KF (2007) Reductive dichlorination of tetrachloroethylene and trichloroethylene by mackinawite (FeS) in the presence of metals: reaction rates. Environ Sci Technol 41:6390–6396
Kennel JR (2008) Advances in rock core VOC analyses for high resolution characterization of chlorinated solvent contamination in a dolostone aquifer (thesis), Waterloo, Ontario, Canada
Lallemand-Barres A, Peaudecerf P (1978) Recherche de relations entre la valeur de la dispersivite macroscopique d'un milieu aquifer, ses autres caracteristiques et les conditions de mesure. Bulletin Bureau de Recherches Geologique et Miniers, France, Section III 2:277–284
Lee W, Batchelor B (2002) Abiotic reductive dichlorination of chlorinated ethylenes by iron-bearing soil minerals. 1. Pyrite and magnetite. Environ Sci Technol 36:5147–5154
Loop CM, White WB (2001) A Conceptual model for DNALP transport in karst ground water basins. Groundwater 39(1):119–127
Lu X, Wilson JT, Kampbell DH (2006) Relationship between Dehalococcoides DNA in ground water and rates of reductive dechlorination at field scale. Water Res 40:3131–3140
National Research Council (1994) Alternatives for ground water cleanup. National Academies Press, Washington, DC
Neuman SP (1990) Universe scaling of hydraulic conductivities in geologic media. Water Resour Res 26(8):1749–1758
Plett JH (2006) Metolachlor and TCE plume characteristics in a dolostone aquifer using a transect (thesis), Waterloo, Ontario, Canada
Randrianarivelo M, Zhou W, Barsa M (2019) Remedial investigations of karst aquifers: a case study at former Marietta Air Force Station, Lancaster County, Pennsylvania. Carbonates Evaporites 34:233–247. https://doi.org/10.1007/s13146-017-0369-y
Terzaghi K, Peck RB, Mesri G (1996) Soil mechanics in engineering practice, 3rd edn. Wiley, New York
Teutsch G, Sauter M (1991) Groundwater modeling in karst terranes—scale effects, data acquisition, and field verification. In: Proceedings of the third conference on hydrogeology, ecology, monitoring, and management of ground water in Karst Terranes, Nashville, Tennessee, December 4–6, 1991. National Ground Water Association, pp 17–54
Tobiszewski M, Namiesnik J (2012) Abiotic degradation of chlorinated ethanes and ethenes in water. Environ Sci Poll Res 19:1994–2006
USEPA (1989) Risk assessment guidance for superfund, volume I: human health evaluation manual (part a) (interim final). Report No. EPA/540/1 89/002. Office of Emergency and Remedial Response, Washington, D.C.
USEPA (1991) Memorandum: human health evaluation manual, supplemental guidance: "standard default exposure factors." Office of Solid Waste and Emergency Response. OSWER Directive: 9285.6-03
USEPA (1992) Guidelines for data usability in risk assessment (part A). Office of Solid Waste and Emergency Response (OSWER), Publication OSWER9285.7-09A
USEPA (2004) Risk assessment guidance for superfund. Volume I: human health evaluation manual (part E: supplemental guidance for dermal risk assessment) final. OSWER. EPA-540-R-99-005
USEPA (2005) Guidelines for carcinogen risk assessment. EPA/630/P-03/001F. Risk assessment forum
USEPA (2013) Regional screening levels summary table and regional screening levels summary table user guide. http://www.epa.gov/reg3hwmd/risk/human/rb-concentration_table/usersguide.htm
USEPA (2014) IRIS (integrated risk information system) database. http://www.epa.gov/iris. Environmental Criteria and Assessment Office, Cincinnati
USEPA (1998) Technical protocol for evaluating natural attenuation of chlorinated solvents in ground water, EPA/600/R-98/128